NAVAL POSTGRADUATE SCHOOL
Monterey, California

THESIS

MESOSCALE SURFACE ANALYSIS OF THE ERICA IOP-5 CYCLONE

by

Susan N. Greer

June 1991

Thesis Advisor Wendell A. Nuss

Approved for public release; distribution is unlimited.

T256960

Unclassified

security classification of this page

REPORT DOCUMENTATION PAGE

1a Report Security Classification: Unclassified		1b Restrictive Markings	
2a Security Classification Authority		3 Distribution Availability of Report: Approved for public release; distribution is unlimited.	
2b Declassification Downgrading Schedule			
4 Performing Organization Report Number(s)		5 Monitoring Organization Report Number(s)	
6a Name of Performing Organization: Naval Postgraduate School	6b Office Symbol (*if applicable*): 35	7a Name of Monitoring Organization: Naval Postgraduate School	
6c Address (*city, state, and ZIP code*): Monterey, CA 93943-5000		7b Address (*city, state, and ZIP code*): Monterey, CA 93943-5000	
8a Name of Funding Sponsoring Organization	8b Office Symbol (*if applicable*)	9 Procurement Instrument Identification Number	
8c Address (*city, state, and ZIP code*)		10 Source of Funding Numbers	
		Program Element No	Project No / Task No / Work Unit Accession No

11 Title (*include security classification*): MESOSCALE SURFACE ANALYSIS OF THE ERICA IOP-5 CYCLONE

12 Personal Author(s): Susan N. Greer

13a Type of Report	13b Time Covered	14 Date of Report (*year, month, day*)	15 Page Count
Master's Thesis	From To	June 1991	74

16 Supplementary Notation: The views expressed in this thesis are those of the author and do not reflect the official policy or position of the Department of Defense or the U.S. Government.

17 Cosati Codes			18 Subject Terms (*continue on reverse if necessary and identify by block number*)
Field	Group	Subgroup	explosive cyclogenesis, surface fluxes, boundry layer

19 Abstract (*continue on reverse if necessary and identify by block number*)

The mesoscale surface structure of an explosively deepening storm that developed during Intensive Observation Period (IOP) 5 (18-20 January 1989) of the Experiment on Rapidly Deepening Cyclones over the Atlantic (ERICA) was examined to determine the influence of surface forcing on explosive cyclogenesis. Aircraft, buoy and ship observations were converted to a 20 km gridded data set in order to generate objective analyses of the surface pressure and temperature fields comparable to the best hand analyses. The Brown-Liu boundary layer model was then used to calculate surface sensible heat fluxes from the gridded data sets. These analyses showed that the most significant feature that distinguished the IOP-5 storm from a typical nonexplosive storm was the region of sustained positive heat fluxes that occurred east of the low center. This feature, combined with substantial warm advection and conditions of moist symmetric neutrality in the baroclinic zone of the warm front, supports destabilization of the boundary layer and enhanced low-level baroclinicity. Thus, the positive heat fluxes fuel the convective transport of heat and moisture to the upper atmosphere and enhance the sensible and condensation heating that contribute to explosive cyclogenesis.

20 Distribution Availability of Abstract	21 Abstract Security Classification	
☒ unclassified unlimited ☐ same as report ☐ DTIC users	Unclassified	
22a Name of Responsible Individual: Wendell A. Nuss	22b Telephone (*include Area code*): (408) 646-2308	22c Office Symbol: MR/Nu

DD FORM 1473,84 MAR

83 APR edition may be used until exhausted
All other editions are obsolete

security classification of this page

Unclassified

Approved for public release; distribution is unlimited.

Mesoscale Surface Analysis of the ERICA IOP-5 Cyclone

by

Susan N. Greer
Lieutenant, United States Navy
B.S., University of Miami, 1981

Submitted in partial fulfillment of the
requirements for the degree of

MASTER OF SCIENCE IN METEOROLOGY AND PHYSICAL OCEANOGRAPHY

from the

NAVAL POSTGRADUATE SCHOOL
June 1991

ABSTRACT

The mesoscale surface structure of an explosively deepening storm that developed during Intensive Observation Period (IOP) 5 (18-20 January 1989) of the Experiment on Rapidly Deepening Cyclones over the Atlantic (ERICA) was examined to determine the influence of surface forcing on explosive cyclogenesis. Aircraft, buoy and ship observations were converted to a 20 km gridded data set in order to generate objective analyses of the surface pressure and temperature fields comparable to the best hand analyses. The Brown-Liu boundary layer model was then used to calculate surface sensible heat fluxes from the gridded data sets. These analyses showed that the most significant feature that distinguished the IOP-5 storm from a typical nonexplosive storm was the region of sustained positive heat fluxes that occurred east of the low center. This feature, combined with substantial warm advection and conditions of moist symmetric neutrality in the baroclinic zone of the warm front, supports destabilization of the boundary layer and enhanced low-level baroclinicity. Thus, the positive heat fluxes fuel the convective transport of heat and moisture to the upper atmosphere and enhance the sensible and condensation heating that contribute to explosive cyclogenesis.

C.1

TABLE OF CONTENTS

I. INTRODUCTION 1

II. BACKGROUND 5
A. ROLE OF SURFACE HEAT FLUXES IN EXPLOSIVE CYCLOGENESIS 5
B. ROLE OF MOIST SYMMETRIC NEUTRALITY 9

III. ANALYSIS 11
A. COLLECTION OF ERICA DATA 11
B. ANALYSIS OF IOP-5 DATA 11
C. BROWN-LIU PBL MODEL 14

IV. SYNOPTIC DISCUSSION OF IOP-5 15
A. 0000 - 1200 UTC 18 JANUARY 1989 16
B. 1200 UTC 18 JANUARY - 0000 UTC 19 JANUARY 1989 17
C. 0000 - 0600 UTC 19 JANUARY 1989 17
D. 0600 - 1200 UTC 19 JANUARY 1989 20
E. 1200 - 1800 UTC 19 JANUARY 1989 22
F. 1800 UTC 19 JANUARY - 0000 UTC 20 JANUARY 1989 24
G. 0000 - 0600 UTC 20 JANUARY 1989 25
H. SUMMARY OF IOP-5 DEVELOPMENT 25

V. BOUNDARY LAYER FORCING 30
A. THERMAL ADVECTION 30
B. ANALYSIS OF SENSIBLE HEAT FLUXES 36
C. AIR-SEA TEMPERATURE DIFFERENCE EVOLUTION AT SELECTED BUOYS 49
D. EVALUATION OF IOP-5 MOIST SYMMETRIC NEUTRALITY 54

VI. CONCLUSIONS AND RECOMMENDATIONS 58

VII. REFERENCES 61

VIII. INITIAL DISTRIBUTION LIST 64

LIST OF TABLES

Table 1. FORECAST ERRORS FOR IOP-5 3
Table 2. CHANGES IN IOP-5 CENTRAL PRESSURE 16
Table 3. BUOY 426E AIR-SEA TEMPERATURE DIFFERENCE 51
Table 4. BUOY 428E AIR-SEA TEMPERATURE DIFFERENCE 52
Table 5. BUOY 433E AIR-SEA TEMPERATURE DIFFERENCE 53

LIST OF FIGURES

Fig. 1. NMC Final 500 mb Height/Vorticity Analysis 18/0000 January 1989 18
Fig. 2. GOES IR Imagery for 18/1801 January 1989 19
Fig. 3. NMC Final 300 mb Height/Isotach Analysis 19/0000 January 1989 20
Fig. 4. IOP-5 Mesoscale Surface Analysis for 19/0300 January 1989 21
Fig. 5. GOES IR Imagery for 19/0601 January 1989 22
Fig. 6. SST Gradients and Track of IOP-5 Cyclone 23
Fig. 7. IOP-5 Mesoscale Surface Analysis for 19/1200 January 1989 24
Fig. 8. IOP-5 Mesoscale Surface Analysis for 19/1800 January 1989 26
Fig. 9. IOP-5 Mesoscale Surface Analysis for 20/0300 January 1989 27
Fig. 10. NMC Final 1000/500 mb Heights and Thickness 20/0000 January 1989 .. 28
Fig. 11. Thermal Advection at 18/2100 UTC January 1989 31
Fig. 12. Thermal Advection at 19/0600 UTC January 1989 32
Fig. 13. NMC Thermal Advection at 19/1200 UTC January 1989 34
Fig. 14. NMC Thermal Advection at 20/0000 UTC January 1989 35
Fig. 15. Sensible Surface Heat Fluxes at 18/1800 UTC January 1989 37
Fig. 16. Sensible Surface Heat Fluxes at 18/2100 UTC January 1989 39
Fig. 17. Sensible Surface Heat Fluxes at 19/0000 UTC January 1989 40
Fig. 18. GOES IR Imagery for 19/0001 January 1989 41
Fig. 19. Sensible Surface Heat Fluxes at 19/0900 UTC January 1989 42
Fig. 20. Sensible Surface Heat Fluxes at 19/1500 UTC January 1989 43
Fig. 21. Sensible Surface Heat Fluxes at 19/1800 UTC January 1989 44
Fig. 22. Sensible Surface Heat Fluxes at 19/2100 UTC January 1989 45
Fig. 23. Air-Sea Temperature Differences at 19/2100 UTC January 1989 46
Fig. 24. Air-Sea Temperature Differences at 20/0300 UTC January 1989 47
Fig. 25. Sensible Surface Heat Fluxes at 20/0300 UTC January 1989 48
Fig. 26. Buoy Air-Sea Temperature Difference 50
Fig. 27. Cross Section at 19/0600 UTC January 1989 56
Fig. 28. Cross Section at 19/0900 UTC January 1989 57

I. INTRODUCTION

Sanders and Gyakum (1980) presented one of the first papers that defined the meteorological "bomb" or rapidly deepening storm and its characteristic climatology, which suggested that the majority of the northern hemisphere's deepest cyclones have been rapidly deepening storms. A rapidly deepening extratropical low is one in which the central pressure at sea level falls at the rate of at least 1 mb h^{-1} for 24 h, a definition attributed to Tor Bergeron. Since this rate was based on a latitude of 60°N, a geostrophically equivalent deepening rate for arbitrary latitudes ϕ is obtained by multiplying this rate by (sin ϕ/sin 60). Using this rate to distinguish nonexplosive from explosively deepening storms, Sanders and Gyakum (1980) found that explosively deepening storms were predominantly maritime, cold season events and were generally found 400 nm downstream from a mobile 500 mb trough. This study also showed that explosively deepening storms occurred over a wide range of sea surface temperatures (SST's) but occurred predominantly near the strongest SST gradients, which suggests an important role for surface interaction. However, numerous studies have identified a variety of factors associated with explosive cyclogenesis.

Upper-level forcing has been shown to be an essential part of the processes that interact with surface processes to result in explosive cyclogenesis. Uccellini et al. (1985) demonstrated that rapid cyclogenesis occurred when high potential vorticity air associated with the upper-level short-wave trough became collocated with the surface low center. Uccellini (1986) noted a similar pattern for the Queen Elizabeth II storm where a distinct short-wave trough and a strong jet streak were aligned with the surface baroclinic zone during the period of rapid deepening. Reed and Albright (1986) examined an eastern Pacific explosive cyclone that formed over a region of weak SST gradients on 13 November 1989. They determined that exceptional cyclonic vorticity was generated at the surface due to strong upward motion in the atmosphere, which was forced by strong and broadly distributed baroclinicity, a jet stream in excess of 90 m s^{-1}, large latent heat release and low static stability (manifested by deep cumulus convection along the northern frontal band and along the upper part of the cold front near the low center). They also noted that the condition for moist symmetric instability (as discussed by Emanuel, 1983) was easily met since weak or neutral stability prevailed throughout most of the depth of the frontal clouds. These results suggest a direct cou-

pling of upper level forcing and surface processes in some explosive cyclones, although the nature and role of the surface processes remains uncertain.

Surface fluxes of latent and sensible heat are presumed to play some role in the baroclinic dynamics of cyclones, but the results of past studies have often been contradictory. Kuo and Low-Nam (1990) studied the effects of surface heat fluxes on cyclone development during model runs initiated at the beginning of the 24 h period of rapid cyclogenesis. They concluded that the fluxes had no significant impact on cyclone development since the model storm deepened at the same rate for both flux and no flux conditions. In contrast, Nuss (1989) conducted a model study which showed that removal of surface heat fluxes, under certain conditions, would result in a significantly deeper storm. These differences may be due to the degree of preconditioning of the atmosphere through warming and moistening prior to cyclogenesis. Nuss and Kamikawa (1990) suggest that the intensity of the influence of surface heat and moisture fluxes may depend on the degree to which the atmosphere has been preconditioned by the fluxes associated with the cold air outbreak of a previous storm. Nuss (1989) suggested that the pattern of surface heat fluxes that produced enhanced cyclogenesis in one of three idealized model experiments would require a preexisting cyclone to the northeast to act as a source of cold air in order to maintain the strong positive fluxes to the northeast of the developing cyclone. The importance of these interactions remains to be demonstrated through observations of actual cyclones.

Early operational numerical models have experienced difficulties in predicting explosively deepening storms and have thus failed to provide adequate early warnings that may have saved lives and property. Sanders and Gyakum (1980) found that, during the cold seasons of 1978 and 1979, the 7-layer National Meteorological Center (NMC) Primitive Equation (PE) global model only captured one third of the mean observed 12-h deepening. In comparison, the NMC Limited-area Fine-mesh Model (LFM) model performed considerably better (Sanders 1986) during the period of 1981-1984 and the model was able to capture 58% of the observed 12-h pressure fall. Further improvements in the ability of operational models to forecast explosive cyclogenesis were noted when Sanders (1987) examined the September 1986 - April 1987 NMC Nested Grid Model (NGM) forecast period, however the specific cause of these improvements is uncertain. Most likely, a combination of factors such as improved analysis, increased horizontal and vertical model resolution and improved model representation of surface and boundary layer fluxes and the effects of cumulus convection contributed to improving the forecasts. Sanders (1987) suggests that a better understanding of why the models perform

as well as they do is key to further improvements. On the other hand, an understanding of the factors that lead to explosive cyclogenesis in actual storms is necessary to provide the ground truth upon which the models are based.

The Experiment on Rapidly Intensifying Cyclones over the Atlantic (ERICA) field study (Hadlock and Kreitzberg 1988) was designed to determine the processes that account for the wintertime phenomenon of explosively developing over-ocean storms. Observations from aircraft, buoys, soundings, satellites and radars were collected during the ERICA field phase from 1 December 1988 to 26 February 1989 for eight rapidly intensifying storms. These data are sufficient to allow examination of the mesoscale features of these storms in order to provide better physical understanding of explosive cyclones as well as ground truth for models. This thesis analyzes the storm that developed during intense observation period (IOP) 5, which occurred 18-20 January 1989.

Further proof of the continuing need for model improvements is demonstrated by examining the quality of the NMC NGM forecast for the IOP-5 storm. Considerable errors were evident when the NGM central pressure forecasts of the IOP-5 cyclone that were valid for 0000 UTC on 20 January 1989 were compared to a 0000 UTC 20 January mesoscale analysis generated well after the experiment. The forecast errors for the 12, 24, and 36 h forecasts are shown in Table 1.

Table 1. FORECAST ERRORS FOR IOP-5

NGM Forecast Valid 0000 UTC 20 January	Central Pressure (mb)	Forecast Error (mb)
12 h	986	1
24 h	998	13
36 h	992	7
0000 UTC 20 January Mesoscale Analysis	985	-

The 24 h forecast underestimated the central pressure by 13 mb which was much worse than the 36 h forecast which only underestimated the pressure by 7 mb. In this case the consistency between consecutive forecasts was poor in addition to poor model forecasts produced for the IOP-5 storm in a single forecast cycle. Consequently, increased understanding of the processes responsible for the explosive development of the IOP-5 cyclone will presumably help to isolate the model deficiencies for this storm.

The overall objective of this study is to provide a relatively complete description of the surface forcing and its possible interaction with significant upper-level processes during the explosive development of the IOP-5 cyclone. Specific objectives are to:

1. Complete a mesoscale surface analysis of the IOP-5 cyclone mean sea level pressure and surface temperature fields using all available observations including surface ships, drifting buoys, P-3 and Electra aircraft observations, satellite imagery and NMC analyses;
2. Describe the upper level forcing including 500 mb short waves, 300 mb jets, and the associated vorticity and divergence to determine their potential role in the cyclogensis of IOP-5 (compare to "typical" patterns);
3. Determine whether the patterns of sensible surface heat flux observed during IOP-5 would tend to enhance or dampen cyclogenetic processes;
4. Assess the potential for surface coupling in a moist neutral or moist symmetrically neutral environment along the warm front;
5. Examine air-sea temperature difference analyses and the relationship between storm center location and Gulf Stream sea surface temperature gradients to determine the influence of sea surface temperatures on boundary layer dynamics and resultant cyclogenesis;
6. Assess the effect that the passage of an earlier storm may have had on the IOP-5 storm and the degree to which "preconditioning" occurred.

II. BACKGROUND

As noted in the introduction, coupling of upper-level forcing and surface effects seems to characterize most explosive cyclones. Davis and Emanuel (1988) indicate that it is difficult to distinguish diabatic processes from other processes that affect the baroclinicity of rapidly developing cyclones. However, they hypothesize that surface heat and moisture fluxes directly couple to upper-level baroclinic processes, because the ascent regions of cyclones are characterized by moist slantwise neutral conditions. In support of this hypothesis, they demonstrate that underprediction of the central pressure of explosively deepening storms is correlated to the reduced 1000-500 mb thickness values (compared to the thickness values characteristic of an atmosphere with a moist adiabatic lapse rate) that characterize regions of explosive cyclogenesis. Furthermore, they suggest that the reduced 1000-500 mb thickness values represent the failure of the NMC LFM to capture the full effects of the surface heat and moisture fluxes. While their climatological correlation is suggestive, the exact nature of the surface interactions that characterize explosive cyclogenesis have yet to be clearly defined.

A. ROLE OF SURFACE HEAT FLUXES IN EXPLOSIVE CYCLOGENESIS

Recently, several studies have indicated that the distribution of surface heat and moisture fluxes plays a critical role in determining the surface flux contributions to cyclogenesis. Nuss and Anthes (1987) completed an idealized cyclone model study that showed that strong upward fluxes in the cold sector and weak downward fluxes in the warm sector weaken the temperature gradient and reduce baroclinicity. This apparent damping effect by an unfavorable heat flux distribution was illustrated when the deepening rate of the model storm increased 25% when the fluxes were removed. In a more detailed examination of three experiments from Nuss and Anthes (1987), Nuss (1989) found that different SST patterns altered the surface heat fluxes, which produced changes in the cyclone deepening rate. The control experiment (Expt. 1) used a zonal SST distribution with positive total heat flux west of the surface low and negative fluxes east of the low. The second experiment (Expt. 2) had the same SST distribution but included no surface heat fluxes while the third experiment (Expt. 3) used a sinusoidal SST distribution and had positive total heat fluxes to the northeast of the surface low as well as to the west of the surface low. Although removal of the surface heat fluxes in Expt. 2 resulted in the deepest most intense surface cyclone, the surface cyclone in Expt.

3 deepened much more rapidly than the full flux control experiment. This suggests that surface heating patterns are critical to determining the role of the surface fluxes in cyclones.

The mechanism by which the pattern of surface heating acts to increase cyclogenesis was also examined by Nuss (1989). Although the static stability for Expt. 3 had decreased over the cyclone center and east of the surface low, the vertical extent of the difference in static stability was not sufficient to explain the large increase in vertical circulation in Expt. 3 compared to the other cases. The effect of the flux distributions on the static stability was limited to the lowest layers of the model which would result in enhanced upward motion only in the very lowest layers. More significantly, Nuss (1989) found that warm frontal convergence increased substantially in the boundary layer of the model. Since the frictional Planetary Boundary Layer (PBL) convergence is proportional to the curl of the surface wind stress (Fleagle and Nuss, 1985) the distribution of the surface wind stress and the curl of the surface wind stress were examined for each of the three experiments. Nuss (1989) found that the wind stress was stronger to the northeast of the surface low and the warm front, which acted to increase the frictional convergence into the surface low and along the warm front. This increase in convergence was associated with an increase in the ageostrophic flow toward the warm front and stronger low-level flow toward the cyclone center. This flow greatly enhanced the transport of heated and moistened air upward into the middle troposphere where it enhanced latent heat release. This effect, due to the differential friction across the warm front, offset the tendency for the heat fluxes to reduce the baroclinicity of the cyclone. Nuss (1989) notes that the pattern of surface heat fluxes that enhanced development requires a source of cold air to the northeast of the developing low, which could be provided by a preexisting cyclone to the northeast of this low.

Nuss and Kamikawa (1990) examined the frictional effect on convergence for an actual explosive and nonexplosive cyclone. The surface heating and moistening to the northeast of the surface low were much more sustained in the explosive cyclone than in the nonexplosive cyclone. For the explosive storm the region of strong positive fluxes to the northeast of the low occurred in the southward flowing branch of a thermally direct circulation associated with the entrance region of the upper-level jet. This circulation maintained strong ageostrophic advection of cold air at the surface and a strong warm front in spite of the tendency to decrease the horizontal temperature gradient by the distribution of surface heat fluxes. This strong, thermally direct circulation did not exist for the nonexplosive storm, which resulted in negative surface heat fluxes to the

northeast of the surface low. As in Nuss (1989), significantly stronger vertical motion occurred along the warm front of the explosive deepening storm, which was potentially due to boundary layer processes similar to those found for the idealized model cyclone.

Results from Nuss (1989), Nuss and Kamikawa (1990) and others illustrate the complex nature of the interaction between surface processes and the dynamics of explosive cyclogenesis and suggest that a simple conceptual cyclone model such as the Norwegian cyclone model (Bjerknes, 1919; Bjerknes and Solberg, 1922) may be too simplified. This model implies surface warm advection to the east of the low and cold advection to the west, which would tend to produce surface cooling by the fluxes east of the low and warming to the west. This pattern would tend to reduce the low-level thermal gradients associated with the fronts.

Fleagle et al. (1988) examined several storms that passed through the Storm Transfer and Response Experiment (STREX) observation region from 1 November to 15 December 1980, which showed observed heat flux patterns similar to those implied by the typical advection patterns for ocean cyclones. The typical distribution of fluxes resulted in reducing the baroclinicty of the frontal regions through heating the cool air west of the fronts and cooling (or warming more slowly) the warm air east of the fronts, which results in conditions apparently unfavorable for development. A closer examination of the boundary layer structure and dynamics indicated that the positive surface heat fluxes in the post-frontal region generated a well-mixed PBL structure, while in the pre-frontal region the boundary layer was more stable leading to a less defined transition zone between the boundary layer and the layer above. This structure is consistent with that found in the model by Nuss (1989) and tends to increase frictional convergence across the fronts.

Results from Neiman et al. (1990) based on observations collected during a storm that occurred during the pre-ERICA test phase confirm this basic pattern of surface interactions in cyclones. The 25-27 January 1988 storm began over warm Gulf Stream waters and then moved over waters that were much colder than the warm sector temperatures, which resulted in fluxes that were directed downward in the warm sector during the period of rapid intensification. Downward fluxes in the warm sector cool the boundary layer and increase its stable stratification as well as weakening the near surface temperature gradient in the frontal zones. This is similar to the structure found by Fleagle et al. (1988). Neiman et al. (1990) also observed that above 900 mb, the warm sector air was not being cooled, and the baroclinicity in the frontal zones at this level was considerably stronger than at the surface. This apparent de-coupling between the

marine boundary layer and the layer just several 100 meters above it may explain why this storm continued to deepen in excess of 1 mb per hour in spite of what appeared to be unfavorable conditions at the surface.

Lilly (1990) examined the surface heat fluxes for the ERICA IOP-2 cyclone that occurred 13-14 December 1988, which provide a counter-example to the typical distribution seen by Fleagle et al. (1988) and Neiman et al. (1990). Mesoscale surface analyses show that during the period of rapid deepening, the IOP-2 low was characterized by strong positive fluxes to the east of the IOP-2 storm with the maximum heating south of the warm front. This flux pattern was strongest prior to the period of rapid development but persisted throughout cyclone development. This pattern of positive heat fluxes to the east of the low center coincides with the Gulf Stream. Nuss and Kamikawa (1990) observed a similar relationship between the Kuroshio and the explosive deepening storm they analyzed. Furthermore, this pattern indicates that strong positive heat fluxes evidently occurred within the baroclinic zone and to its north for both of these studies. This pattern would tend to destabilize a moist symmetrically neutral environment in the frontal region. Lilly also noted that satellite imagery of the IOP-2 storm showed strong convection south and east of the developing cyclone, a pattern observed by Nuss and Kamikawa (1990) as well. This also supports the interpretation that the fluxes are destabilizing a neutral environment.

Most of these previous studies do not address the time evolution of the surface forcing by the surface fluxes and associated boundary layer processes or the degree to which the air may be preconditioned by the fluxes. Kuo and Low-Nam (1990) conducted a series of 14 numerical experiments to identify the key factors that are important to short-range prediction of explosive cyclones. Four of these experiments were designed to test the impact of surface energy fluxes on storm development. The experiments were initialized at the beginning of the 24 h period of rapid development and showed that the fluxes had very little impact on the storm development and in fact, the storms were slightly stronger when the fluxes were removed. These results either contradict those of Davis and Emanuel (1988), which suggest that better parameterization of surface fluxes in the model they examined could have produced a stronger storm, or indicate that the effects of significant preconditioning of the boundary layer air were already present in the initial state used by Kuo and Low-Nam (1990). Since the study conducted by Davis and Emanuel (1988) was initiated 12-24 h earlier than the Kuo and Low-Nam (1990) study it is likely that preconditioning was important. In a follow-on study, Kuo et al. (1991) initiated their model 24 h prior to the 24 h period of rapid cyclogenesis and con-

ducted 48 h model runs. Their results confirmed that fluxes occurring during the earlier period had a much greater effect on the storm development. Kuo et al. (1991) suggest that fluxes during the earlier period increase the "potential" for explosive development and that earlier fluxes contribute to later deepening by providing latent heat for subsequent release in storm clouds. Moreover, a substantial delay may exist between the time when the moisture is evaporated from the ocean surface and when its latent heat is released in frontal clouds. Given these findings, it is clear that the impact of surface fluxes on cyclone development cannot be judged soley from their effect during the rapid deepening stage. Fantini (1990) conducted a theoretical model study of the influence of ocean heat and moisture fluxes on the development of baroclinic waves that supports this hypothesis. He noted that the atmosphere can store the thermal energy received at the air-sea interface in the form of latent heat and subsequently release this energy at a different location as determined by the dynamics.

In summary, the results of both model experiments and the analysis of actual storms indicate that strong surface heat fluxes are characteristic of explosively deepening storms. The preceeding discussion suggests that the degree of influence and the specific role of surface heat fluxes in causing explosive cyclogenesis is still uncertain, but depends on the timing, duration and distribution of the fluxes related to the warm frontal region of cyclones.

B. ROLE OF MOIST SYMMETRIC NEUTRALITY

As suggested by various studies of the surface heat flux influence on explosive cyclones, direct coupling of surface processes to upper level processes occurs when the frontal region is characterized by moist symmetric neutrality. Emanuel (1983) discusses a type of instability known as conditional symmetric instability, where the combination of gravity acting in the vertical direction and centrifugal motion acting in the radial direction results in slantwise convective motion. Consequently, an atmosphere stable to vertical displacements may be unstable to slantwise diplacement, such that convection could still occur in a "traditionally" stable atmosphere. Since warm fronts are moist baroclinic regions, Emanuel (1983) hypothesizes that moist slantwise convection exists in these regions and tends to maintain a condition close to moist symmetric neutrality. Emanuel (1988) evaluated the potential for slantwise convective adjustment in several explosively deepening storms based on measurements from aircraft flown along the M-surfaces. The cross sections using the flight observations collected along the M-surfaces showed large regions neutral to slantwise convection and only small regions of instabil-

ity, which supports the hypothesis that slantwise moist convection is continuously neutralizing the instability generated by large scale ascent.

Davis and Emanuel (1988) suggest that the conditions of slantwise neutraility observed by Emanuel (1988) support the growing evidence that the environment of midlatitude cyclones may be characterized by zero moist potential vorticity q_e, which is equivalent to the statement that a parcel lifted along an M-surface would have zero buoyancy and be stable to vertical displacements. This condition would suggest a susceptibility for slantwise convection in the presence of suitable environmental forcing, such as surface heating and moistening, but would imply a stable vertical lapse rate and no vertical convection. Davis and Emanuel (1988) propose that the strong positive heat fluxes that usually occur in regions of explosive cyclogenesis provide the forcing needed to generate and maintain slantwise convection. Nuss and Kamikawa (1990) and Kuo and Low-Nam (1990) both provide support for this hypothesis.

Nuss and Kamikawa (1990) used available sounding data to construct cross sections that show slantwise neutrality in the frontal zone and symmetric instability south of the front for an explosive cyclone and nonexplosive cyclone. Satellite imagery of both storms showed convective activity in the warm frontal regions, indicating that slantwise convection could have occurred in both cases. Nuss and Kamikawa (1990) suggest that the differences in the deepening rates of the two storms potentially resulted from continuous strong positive fluxes, which produced conditions favoring moist convective adjustment throughout the development of the explosively deepening storm.

Kuo and Low-Nam (1990) presented further evidence that moist symmetric neutrality may be a common feature of explosively deepening storms in numerical models as well. Their model simulation that produced the most realistic cyclone development showed that the warm frontal region was characterized by moist symmetric neutrality, which suggests that this condition may be a salient feature of rapidly developing cyclones. However, as noted in the previous section, not all explosive cyclones have sustained surface fluxes to destabilize the frontal region, which suggests that this characteristic may not be necessary in all explosive cyclones.

III. ANALYSIS

A. COLLECTION OF ERICA DATA

The ERICA field study was designed to collect data at the time and spatial scales necessary to allow examination of the dynamics that lead to rapidly intensifying storms. Hadlock and Kreitzberg (1988) describe plans for the ERICA field phase. Aircraft measurements formed the core of the ERICA field measurement program since aircraft have the flexibility to deploy quickly and collect observations in the critical regions of a storm. A United States Air Force (USAF) WC-130, the National Center for Atmospheric Research (NCAR) Sabreliner, two National Oceanic and Atmospheric Agency (NOAA) WP-3D, Navy P-3, NCAR Electra, and commercial aircraft all contributed to the data collection effort at different phases of the project. The majority of aircraft observations used for the IOP-5 analysis were collected by the two NOAA WP-3D aircraft which conducted three flights on 19 January 1989 and one on 20 January. The remainder of the aircraft observations were collected during one Electra flight on 19 January. The buoy data collection system for the experiment included the current operational moored buoys, several special moored buoys and up to 100 air-deployed drifting buoys. For the IOP-5 time period only 13 drifting buoys that were dispersed through the central area of the IOP-5 observation region were available for analysis. Ships of opportunity, the existing land-based sounding network and supplemental rawindsonde soundings at 1, 3 and 6 h intervals completed the surface data set collected during ERICA. Geostationary Operational Environmental satellite (GOES) imagery was available to aid in the synoptic analysis and NOAA Advanced Very High Resolution Radiometry (AVHRR) provided the 10 day composite SST analysis used in this study.

B. ANALYSIS OF IOP-5 DATA

As mentioned in the previous section, the observations used for the analysis of IOP-5 were collected by P-3 and Electra aircraft, moored and drifting buoys, ships of opportunity and land-based stations. Aircraft observations were collected continuously throughout the 8-9 h missions. Although the aircraft observations provide a detailed picture of the mesoscale structure of the low center and the frontal regions, their continuous and asynoptic character make them difficult to use in synoptic analyses. To address this problem, these continuous 1 s observations were combined into discrete observations by averaging over 30 s intervals. To guarantee quality observations, data

taken during significant turning or climbing of the aircraft were excluded. For most of the analyses, the aircraft observations were further filtered so that only every 15th observation was retained to make the frequency of the observations consistent with the resolution of the model analysis grid. It was also necessary to reduce the aircraft data to the surface in order to provide data usable for a surface analysis. This was done by setting an arbitrary ceiling of 1000 m and disregarding all observations above that level. The temperature was reduced to the surface by assuming a moist adiabatic lapse rate, $\gamma = 6.5°$ C km^{-1}, which is a reasonable assumption since convective clouds were often present throughout the area of interest. The pressure data were reduced to the surface using the hypsometric equation.

To correct for the asynoptic character of the aircraft observations they were translated such that observations before and after the analysis time (within each 3 h interval) were relocated to positions that would approximate the positions they would have held at the analysis time. The translation speed was calculated by estimating the 6 h speed and direction of movement of the surface low from the Sanders (1989) analyses. Sanders (1990) compared his hand analyses to the NMC manual and automated analyses and he considered his analysis to be the ground (or sea) truth due to the larger data base, later preparation time and lack of operational deadlines. Consequently, the cyclone movement is considered essentially correct for this calculation. The time difference between the observation and the analysis was then used to calculate a new position for the observation at the analysis time. This method assumes that the cyclone is quasi-steady state over the time of translation, which is clearly not true for explosive cyclogenesis, and also neglects the effect of the motion of the fronts relative to the cyclone center. Still, the application of this correction greatly improved the consistency of the observation points and generated a more realistic analysis.

The Cressman (1959) objective analysis method was used to convert the irregularly spaced observations into gridded data points. The Cressman method applies successive corrections to a first guess field where the corrections are based on a weighted sum of the differences between the interpolated value of the first guess and the nearby observation points. The weighting factors are determined from the square of the distance between each grid point and observation. Data for the analysis included all available marine and land-based surface observations plus the translated aircraft observations in each 3 h interval from 1800 UTC 18 January to 0600 UTC 20 January 1989. For the IOP-5 data analyses, the first guess field used for the first analysis at 1800 UTC 18 January was the NMC Final Analysis field for 1200 UTC 18 January. Subsequent analyses

used the gridded data output from the previous time period as the first guess. Successive corrections were applied during 5 passes through the data with the radius of influence ranging from an initial scan radius of 10.0 grid lengths to a final radius of 1.7 grid lengths. The resultant 80 km gridded data set was used to generate objective (computer generated) analysis fields of temperature and pressure for each 3 h time period. Lack of an adequate number of reliable dewpoint observations prevented the analysis of the dewpoint temperature field, and uncertainty in the reduction of the aircraft winds to the surface prevented the completion of a wind analysis. Thus, the contribution of variations in atmospheric moisture to the boundary layer forcing was not specifically examined in this study. The fields were then corrected by adding bogus observations and rerunning the objective analysis routine to generate an analysis that would closely resemble the best subjective analysis (in this case the Sanders (1989) analyses) that could be produced using this data field. The 80 km analyses were interpolated to a 20 km grid for computation and plotting purposes. Final adjustments were made to the 20 km gridded analysis fields (by running the analysis again as necessary) to guarantee consistency in time and space as well as agreement with the GOES imagery of the IOP-5 storm.

Several methods were used in this study to yield accurate objective gridded fields. First, the consistency of the observations, particularly the drifting buoy observations was checked by examining their reports over time and comparing them to the first guess analysis. In particular, five drifting buoys in the vicinity of the storm center were closely examined and it was found that the pressure observations were consistent over a period of 24 h and that the buoy pressure observations agreed closely with the surrounding observations and the analysis pressures. This result agrees with Sanders (1990) who reported that, on the whole, buoy performance was good, but that some buoys had consistent 1-3 mb errors while others exhibited increasing errors just before "dying" or even intermittent errors. Next, observations that were plotted on the 6 hourly Sanders (1989) analyses but that did not appear in the ERICA data set were added to the IOP-5 data sets. These were probably either delayed ship observations referred to by Sanders (1990), which failed to be included in the ERICA data set, or observations in the domain outside the ERICA observation area. The ERICA observation area only included data west of 50° W and north of 30° N, while the analysis grid used in this study extends further east and south. Finally, additional "bogus" points were added to produce a Cressman analysis of the pressure and temperature fields that agreed with the Sanders (1989) hand analyses. These additional points were used to increase or decrease gradients, position

isolines more parallel to fronts (located by satellite imagery) or fill in data in data sparse areas.

C. BROWN-LIU PBL MODEL

The boundary layer dynamics of the IOP-5 storm are examined using the marine planetary boundary layer (PBL) model developed by Brown and Liu (1982). This model determines surface winds and stress in the PBL from the surface winds at the top of the PBL by including surface roughness feedback, variable humidity, and interfacial layer effects. The program uses the synoptic-scale pressure field to calculate the surface geostrophic flow and then corrects for isobar curvature effects to determine the gradient wind, which serves as the upper boundary condition. The Brown-Liu PBL model is a matched two-layer model where the outer layer is an Ekman/Taylor layer with stratification-dependent secondary flow providing a variable mean profile. Thermal wind corrections are included in this layer. The surface layer is logarithmic and corrected for stratification effects, humidity effects and variations in surface roughness. The solution in the two layers is then matched at the interface between the layers. The model generated surface wind fields are solved for iteratively, based on an estimate of the surface friction velocity and fluxes. Consequently, the estimate of the friction velocity and the sensible and latent heat fluxes from the available temperature and moisture fields is used to generate the sensible heat flux and surface stress fields for IOP-5. Since reliable moisture (dewpoint temperature) fields could not be generated from the IOP-5 data as noted above, the latent heat flux fields were calculated with an assumed constant relative humidity of 70%. This value was a reasonable average for the region of convective activity and precipitation present throughout the IOP-5 storm, but provides no information about spatial variability of the moisture flux beyond that implied by the temperature distribution. Consequently, the latent heat flux fields were not used for any diagnosis of the forcing by the moisture flux.

IV. SYNOPTIC DISCUSSION OF IOP-5

The IOP-5 storm which developed 18-20 January 1989 was an explosively deepening storm with a maximum deepening rate of 32 mb over 24 h. A 500 mb trough and its associated strong vorticity maximum were positioned upstream of the developing storm and two substantial 300 mb jets (80 kt) diverged in the same location creating a region of diffluence above the developing low. The 500 mb trough and 300 mb jets were both in a position to provide favorable upper-level forcing. A preexisting storm that was located northeast of the developing IOP-5 low (over Quebec) was positioned such that its northerly cold advection could contribute to the air-sea temperature differences that exist over the Gulf Stream. This region is characterized by cooler surface air temperatures above the warmer Gulf Stream. This relationship initiated positive heat fluxes which possibly preconditioned the atmosphere in the region where the storm would develop. The IOP-5 surface low initially developed off the coast of North Carolina above the strong SST gradient associated with the Gulf Stream, and continued to remain within the influence of the Gulf Stream SST gradient throughout development. The surface wind patterns indicate the presence of strong warm advection east of the low center and the Brown-Liu boundary layer model indicates that strong positive surface sensible heat fluxes were present east of the IOP-5 storm center throughout development.

Lilly (1990) analyzed an earlier ERICA storm, IOP-2, which developed 13-14 December 1988. His results are summarized here, but more detailed descriptions are referenced later when they appear relevant to the IOP-5 analysis. Since both storms developed in nearly the same geographic region, it is possible that their similarities as well as their differences will provide insight into the dynamics of explosive cyclogenesis.

Prior to development of the IOP-2 storm a preliminary (or preexisting) low moved off the coast of Florida early on 13 December 1988 and continued to develop, although not explosively, as it moved toward the northeast. A strong short-wave trough initiated development of the IOP-2 storm to the northwest of the preexisting storm. The IOP-2 low developed in an area of strong sea-surface temperature gradients associated with the Gulf Stream and was supported by strong upper-level vorticity advection during the rapid deepening period. The IOP-2 low was also characterized by weak surface warm advection to the east since the preexisting storm to the southeast inhibited the low level circulation. In spite of this weak advection, the regions east and northeast of the low

experienced large increases in the surface air temperatures, suggesting strong positive heat fluxes from the ocean. The IOP-2 storm deepened 19 mb during its 6 h period of most rapid development, with a maximum deepening rate of 40 mb over 24 h. In comparison, Table 2 shows that the IOP-5 storm deepened 14 mb during its 6 h period of most rapid development, with a maximum rate of 32 mb over a 24 h period. This would suggest that the IOP-2 storm was somewhat more intense than the IOP-5 storm. Lilly (1990) also included a table summarizing the development of IOP-2 in which he listed the low central pressures at 3 h intervals. It is interesting to note that both tables suggest a similar pattern of development where a 9 h period of rapid development is both preceded and followed by periods of more modest intensification.

Table 2. CHANGES IN IOP-5 CENTRAL PRESSURE

Date Time (UTC January 1989)	Central Pressure (mb)	Previous 3 h Change	Previous 6 h Change
19/0000	1015	-	-
19/0300	1012	3	-
19/0600	1010	2	5
19/0900	1006	4	6
19/1200	1004	2	6
19/1500	1002	2	4
19/1800	994	8	10
19/2100	988	4	14
20/0000	985	3	9
20/0300	980	5	8
20/0600	978	2	7
20/0900	974	4	6
20/1200	971	3	7

A. 0000 - 1200 UTC 18 JANUARY 1989

The NMC Final sea-level pressure analysis for 0000 UTC 18 January (not shown) indicates a preexisting low center with a central pressure of 1009 mb located over Quebec (hereafter, date and time UTC will be denoted by day/hour, e.g. 18/0000). By 19/0000 January this surface low will become vertically stacked with the upper-level 500 mb

trough axis and the associated vorticity maximum (at 18/0000, Fig. 1 shows this axis centered over Maine). As the 500 mb trough moves east of the surface low, conditions become unfavorable for further development. The path of movement of this storm will eventually place it northeast of the IOP-5 storm in a position where its circulation of cold air could affect the circulation and development of the IOP-5 storm. A second 500 mb trough (Fig. 1) is located over the central United states with a relative vorticity maximum of 12 x $10^{-5}s^{-1}$ centered above North Dakota. This upper-level trough provides the forcing that initiates development of the IOP-5 surface low off the Carolina coast. The 18/0000 January NMC Final 300 mb isotach analysis (not shown) shows a jet with a 120 kt core southeast of Newfoundland. This jet has a split tail with 80 kt branches trailing over New York to the north and Georgia to the south. The IOP-5 surface low develops in the area between these two jets.

B. 1200 UTC 18 JANUARY - 0000 UTC 19 JANUARY 1989

The 18/1200 January NMC Final 500 mb analysis (not shown) indicates that the 500 mb trough has deepened and its associated relative vorticity maximum has increased to $15x10^{-5}s^{-1}$. The axis of the trough has moved eastward and is now centered over Iowa. This configuration suggests favorable upper-level support, positive vorticity advection (PVA) and divergence, ahead of the trough moving toward the region where the IOP-5 cyclone develops. The preexisting low center over Quebec has moved offshore and deepened slightly to 1007 mb.

Weak confused winds are evident along the Carolina coast, as indicated by the 18/1800 mesoscale analysis (not shown), while stronger 15 kt southeasterly winds are evident off the Florida coast. GOES IR imagery for 18/1801 (Fig. 2) shows clouds over the Gulf Stream which correspond to the area of PVA and divergence associated with the eastward moving 500 mb trough. By 18/2100 January the mesoscale analysis (not shown) indicates that the winds off the Carolina coast have increased to 15-20 kt from the south and the surface air temperature gradient is parallel to the Gulf Stream. These cross-gradient winds indicate that warm air is being advected into this region.

C. 0000 - 0600 UTC 19 JANUARY 1989

The 19/0000 January NMC Final 500 mb analysis (not shown) indicates that the 500 mb trough has continued to deepen and its vorticity maximum is now $18x10^{-5}s^{-1}$. The trough axis is now located over Georgia and Ohio, and the PVA and divergence ahead of the trough are located above the region where the surface low has begun to form. The 19/0000 January mesoscale analysis (not shown) indicates a low pressure area (not

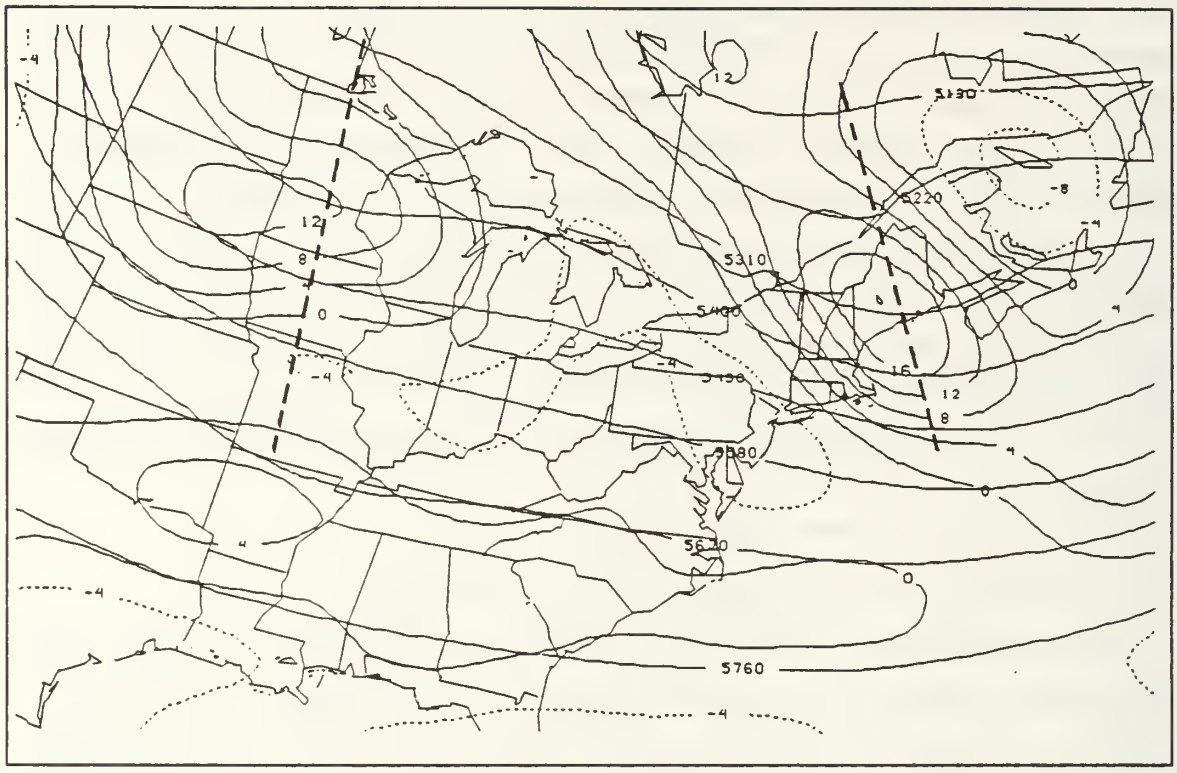

Fig. 1. NMC Final 500 mb Height/Vorticity Analysis 18/0000 January 1989: Units of height are m and units of relative vorticity are $10^{-5}s^{-1}$. Dashed lines mark axes of 500 mb troughs.

closed) of 1015 mb off the coast of North Carolina. The GOES IR imagery for 19/0301 (not shown) indicates that convective clouds with cold cloud top temperatures have formed into a "frontal wave" shape and their location corresponds to that of the surface low. By 19/0401 GOES IR imagery (not shown) indicates that the cloud top temperatures have become colder and the distribution of clouds more extensive.

At 19 0000 January a well organized 300 mb jet with a 100 kt core has developed over North Carolina and Virginia (Fig. 3). This 100 kt jet splits into two 80 kt jets that diverge north and south of the surface low, which develops in the region of diffluence between the two jets. This configuration implies enhanced upper level divergence and should lead to enhanced cyclone development.

South of the newly formed low center, the 19/0000 mesoscale analysis (not shown) depicts southerly winds of 15-20 kt. Warm advection has forced the temperature gradient to the north resulting in the typical frontal wave pattern that forms a sector of warm air

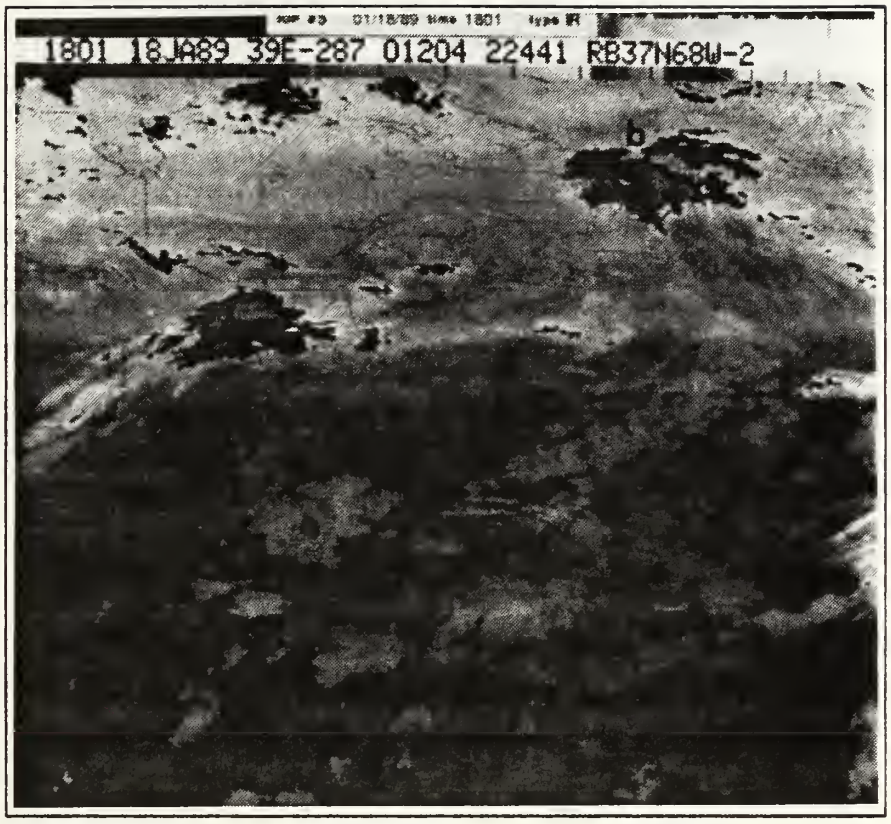

Fig. 2. **GOES IR Imagery for 18/1801 January 1989:** Letter a identifies cloud mass associated with incipient IOP-5 disturbance and letter b identifies location of preexisting storm.

to the southeast of the developing low. The 19/0300 mesoscale analysis (Fig. 4) shows that the low center, although still not closed has deepened to 1012 mb. GOES IR imagery at 19/0401 (not shown) indicates that the northern edge of the cloud mass of the developing warm front is parallel to the surface thermal gradient. The 19/0300 analysis (Fig. 4) also shows weak 5-10 kt southeasterly winds north of the developing warm front with cyclonic turning of the winds evident around the developing low center and the thermal gradient parallel to the warm front. It should be noted that the figures representing the IOP-5 mesoscale analysis are smaller than the 13x13 inch plots used to generate the analyses and do not include all available observations. The isotherms and isobars are plotted based on the entire data field, but the observations were filtered to produce a readable plot. The flow around the preexisting cyclone, now located to the

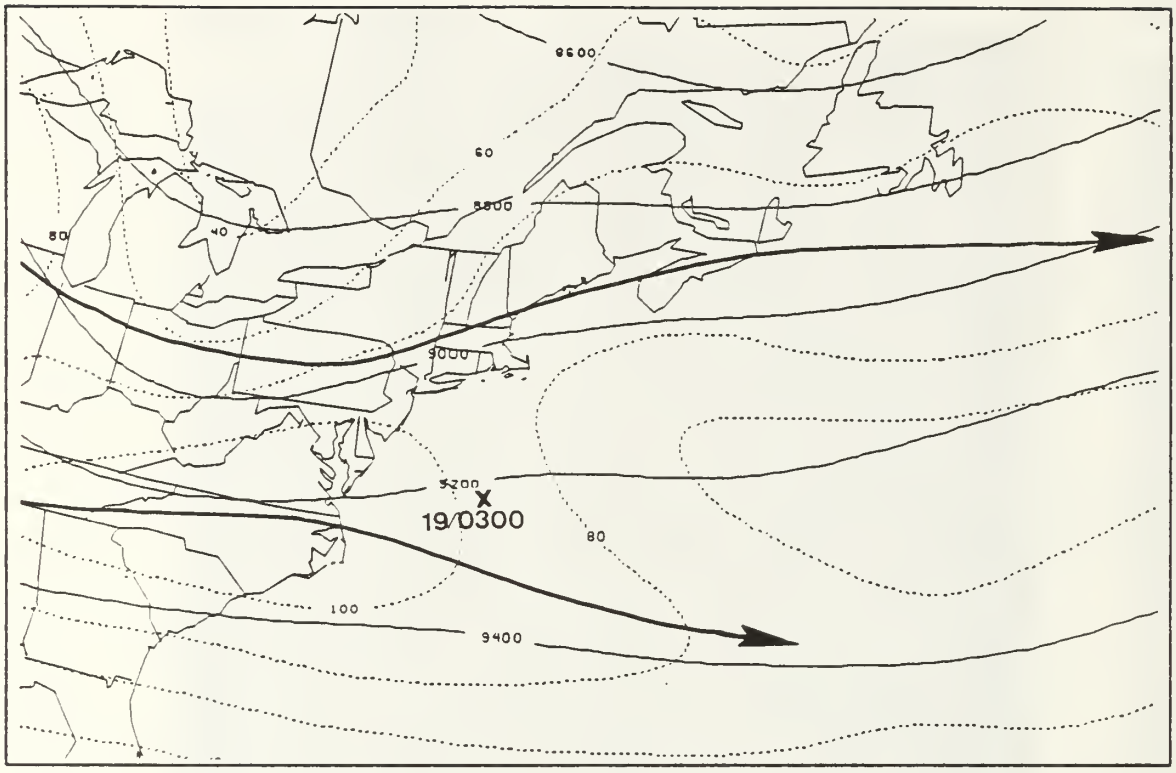

Fig. 3. NMC Final 300 mb Height/Isotach Analysis 19/0000 January 1989: Units of height are m and units of speed are kt. Heavy solid lines indicate location of 300 mb jet axis. An x marks the location of the developing surface low center at 19/0300.

northeast of Newfoundland, does not appear to be directly influencing the circulation of the developing IOP-5 low.

D. 0600 - 1200 UTC 19 JANUARY 1989

GOES IR imagery for 19/0601 (Fig. 5) shows that the convective clouds associated with the IOP-5 storm have become more extensive and are beginning to evolve toward the comma shaped expected according to the conceptual model for cyclone development. Southerly winds of 20-30 kt are seen in the warm sector of the developing low on the 19/0600 mesoscale analysis (not shown) indicating increased warm advection. The isobars around the low center are still not closed but the low has deepened to 1010 mb. The SST analysis (Fig. 6) shows that the low center is located in a region of the strong SST gradient associated with the Gulf Stream. Furthermore, the surface air temperature isotherms are parallel to the Gulf Stream SST gradient and thus, parallel to the warm

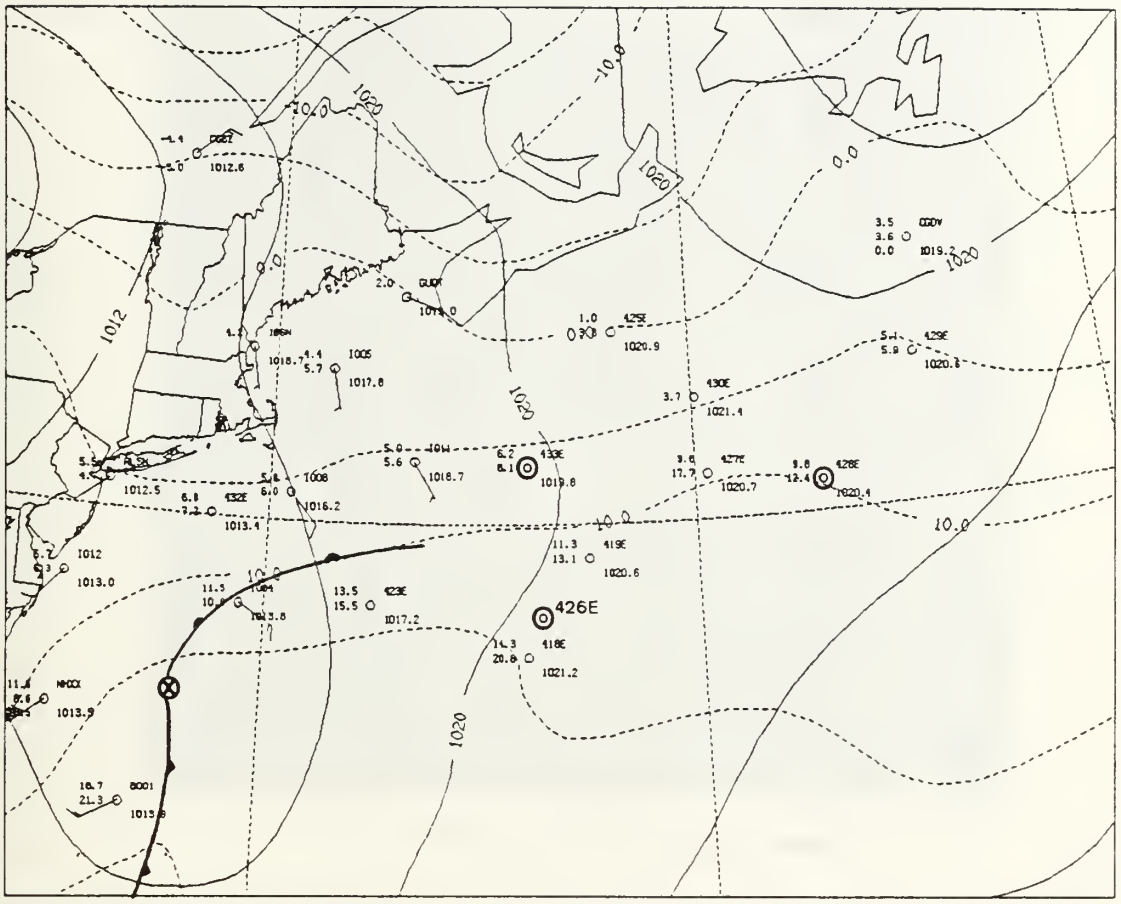

Fig. 4. IOP-5 Mesoscale Surface Analysis for 19/0300 January 1989: Solid lines are surface isobars at 4 mb intervals and dashed lines are isotherms of surface air temperature at 5° C intervals.

front, but not parallel to the cold front. At this stage the Gulf Stream apparently has a stonger influence on the surface air temperatures than the circulation associated with the developing cold front. In spite of this weak surface temperature gradient, the GOES imagery for 19/0601 (Fig. 5) shows a band of clouds extending southward from the comma head that represents the cold front, while the surface wind observations show a shift from northwesterly to southwesterly winds across the cold front as indicated by the satellite imagery.

The 19/0900 January mesoscale analysis (not shown) shows that the low center is now closed and has moved northeast along the north wall of the Gulf Stream and the region of strongest SST gradient. The 20-30 kt northwesterly winds in the cold sector indicate that cold advection is taking place in spite of the weak thermal gradient in the

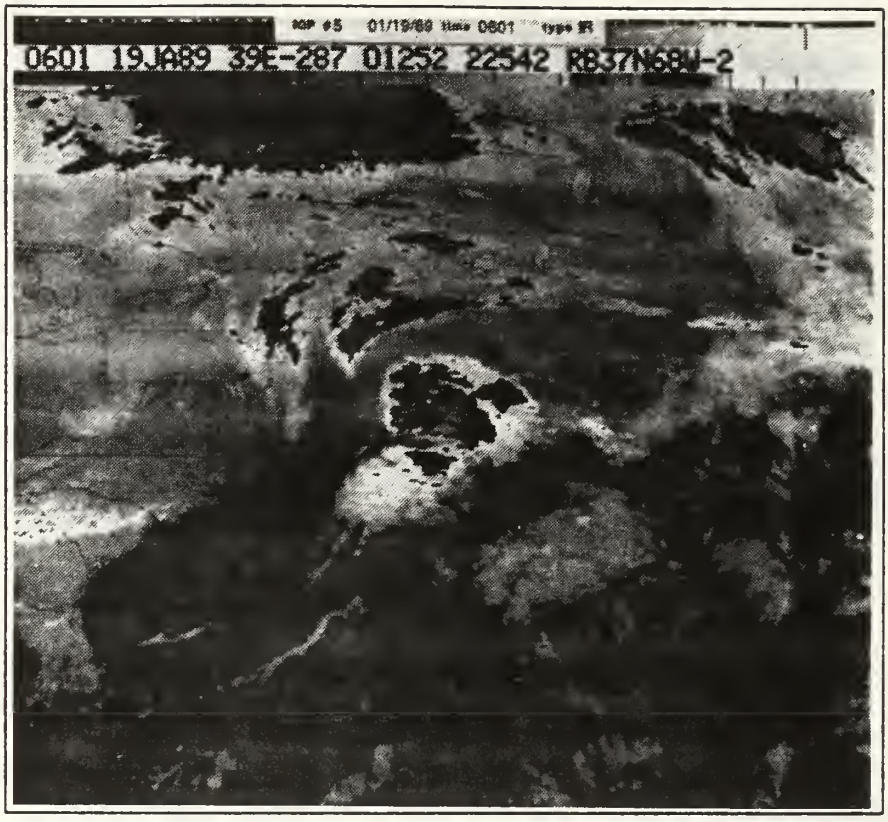

Fig. 5. GOES IR Imagery for 19/0601 January 1989

cold frontal region. Aircraft observations show a strong wind shift that clearly defines the location of the warm front, with easterly winds ahead of the warm front nearly parallel to the thermal gradient. The low has deepened to 1006 mb and GOES IR imagery for 19/0901 (not shown) indicates that the circulation has intensified and that the size of the cloud mass has increased.

E. 1200 - 1800 UTC 19 JANUARY 1989

The 19/1200 NMC Final 500 mb analysis (not shown) indicates that the axis of the 500 mb trough and its strong vorticity maximum ($20x10^{-5}s^{-1}$) have moved eastward and are now centered at 38° N, 72° W. This allows the favorable upper level support to continue, since the PVA and divergence ahead of the 500 mb trough are located above the developing surface low. The 19/1200 NMC Final 300 mb analysis (not shown) indicates that the 300 mb jet core has increased in strength to 120 kt and now extends from Ohio and Virginia out over the Atlantic ocean south of the developing low. The surface low center is now located beneath the left exit region of the jet where upper level diver-

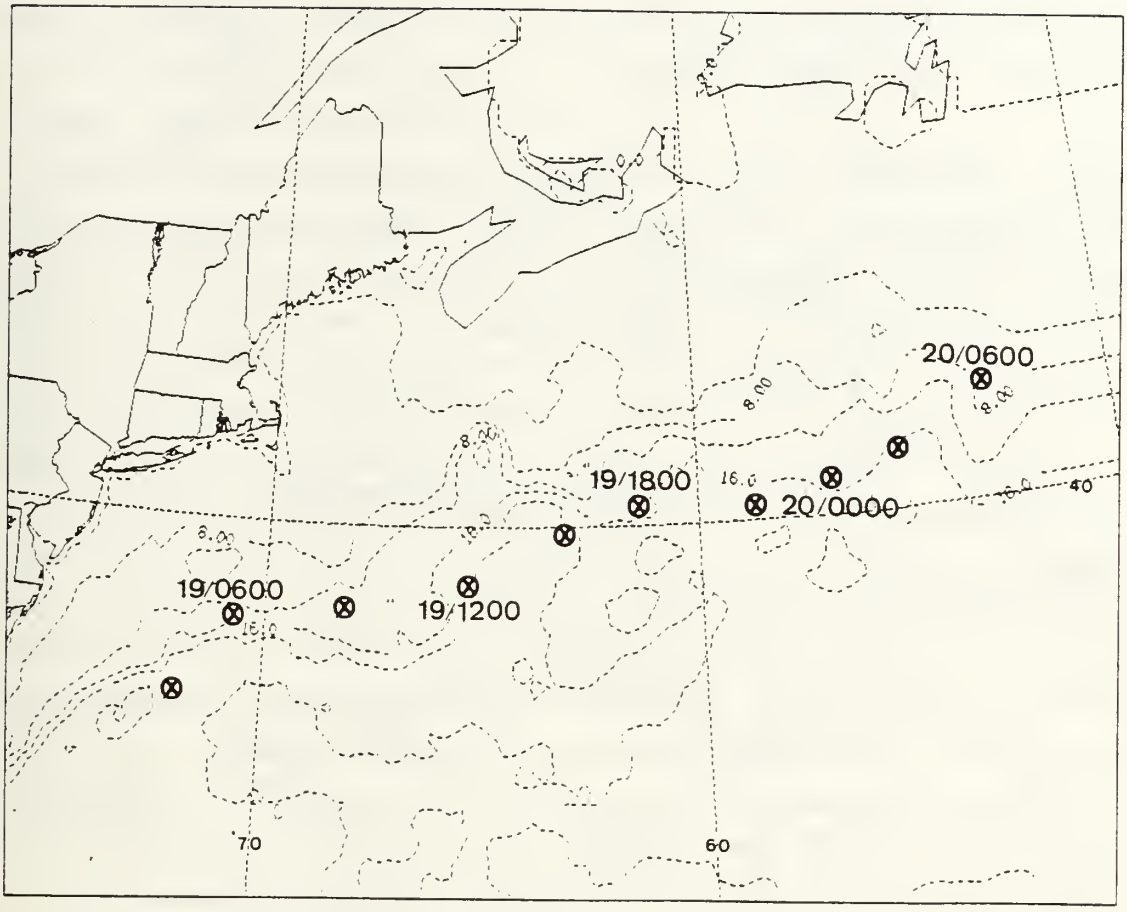

Fig. 6. SST Gradients and Track of IOP-5 Cyclone: Track of IOP-5 cyclone is marked at 3 h intervals from 19/0300 - 20/0600 January 1989. Sea surface temperature isotherms based on NOAA AVHRR data are at 2° C contour interval.

gence should enhance development. The 19/1200 mesoscale analysis (Fig. 7) shows continued easterly flow ahead of the warm front with 10-15 kt winds parallel to the thermal gradient, while winds in the warm sector have increasd to 20-25 kts and a strong cyclonic circulation is evident. The low central pressure has deepened to 1004 mb and GOES VIS imagery for 19/1401 (not shown) verifies the continuing intensification of the IOP-5 storm. By 19/1500 the mesoscale analysis (not shown) indicates that the low has deepened to 1002 mb and that strong 35 kt winds are evident in the region of the warm front, suggesting that the storm circulation has strengthened considerably. This time marks the beginning of the period of most rapid cyclogenesis during which the central pressure will deepen 14 mb during the next 6 h.

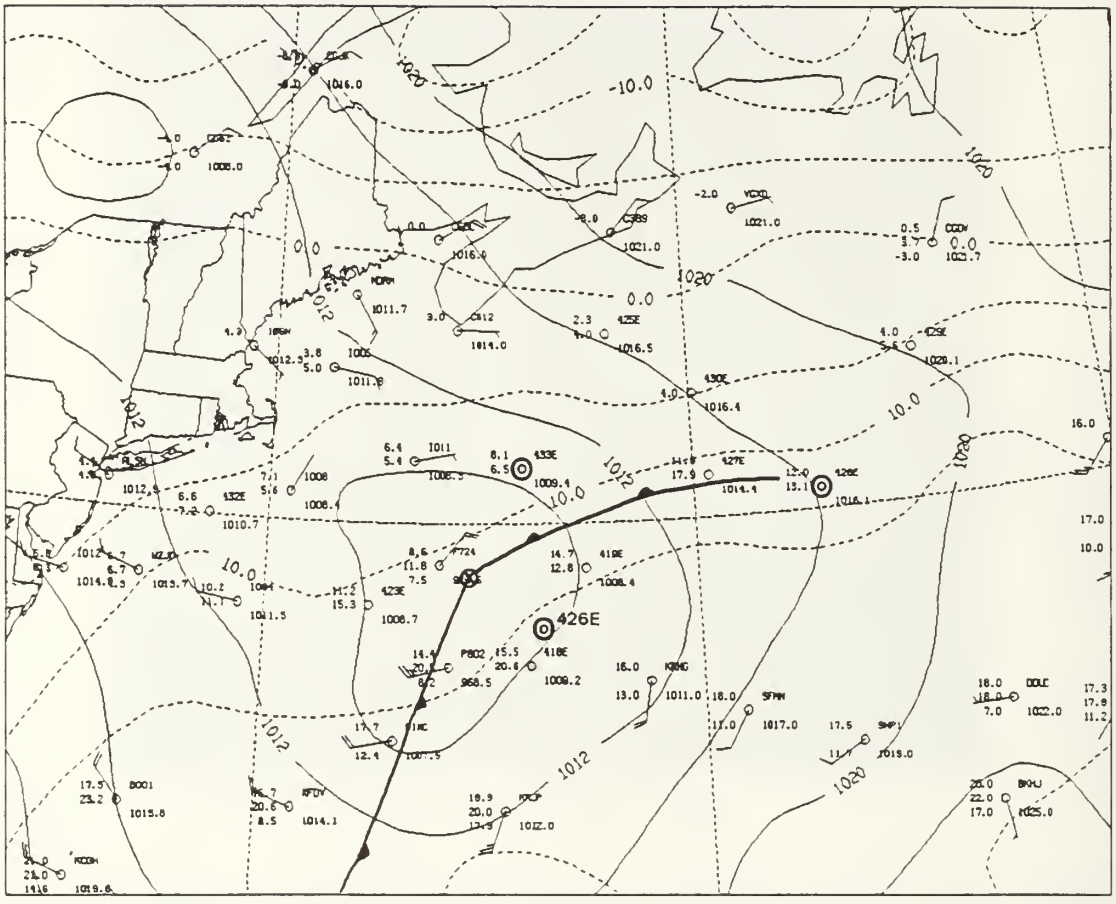

Fig. 7. IOP-5 Mesoscale Surface Analysis for 19/1200 January 1989: Same as for Fig. 4.

F. 1800 UTC 19 JANUARY - 0000 UTC 20 JANUARY 1989

At 19/1800 the strong pressure gradient and 40 kt winds shown on the mesoscale analysis (Fig. 8) are characteristic of a strong cyclonic circulation. The surface air temperature isotherms are still parallel to the Gulf Stream with a strong gradient associated with the warm front and a weaker gradient west of the cold front. The low has deepened to 994 mb, a drop in pressure of 8 mb over 3 h, and the low continues to deepen rapidly so that by 19/2100 the mesoscale analysis (not shown) indicates the pressure has dropped an additional 6 mb to 988 mb. At this time the low center is located over a region of weaker SST gradient but has continued to move parallel to the Gulf Stream. Surface observations to the east of the cyclone are becoming more sparse as the cyclone center approaches the edge of the ERICA observation area, but aircraft observations clearly show the location of the low center and the warm front. GOES IR

imagery at 19/2301 (not shown) indicates that the fronts are beginning to occlude, since the clouds associated with the comma head are beginning to wrap around the low center.

G. 0000 - 0600 UTC 20 JANUARY 1989

The NMC Final 500 mb analysis for 20/0000 January (not shown) indicates that the amplitude of the 500 mb trough has increased and its vorticity has increased as well to $25x10^{-5}s^{-1}$. The trough axis has continued to propagate eastward and is now centered at 35° N, 58° W. The NMC Final 300 mb analysis for 20/0000 January (not shown) indicates that the 300 mb jet, with its extended region of strong 100 kt winds, remains in a position favorable to enhance cyclogenesis since the eastward motion of the surface low has continued to place it beneath the left exit region of the jet.

The mesoscale analysis for 20/0300 January (Fig. 9) shows that the central pressure has deepened to 980 mb and that strong winds up to 45 kt are present north of the warm front. The surface air temperature gradient remains strong along the warm front and is beginning to develop parallel to the cold front within the cold sector as well. The strong cyclonic circulation within the cold sector, indicated by the strong pressure gradient and 40-45 kt winds, appears to have finally overcome the influence of the Gulf Stream SST gradient so that cold advection has begun to move the thermal gradient more parallel to the cold front. Strong 45 kt winds and a similar thermal structure are also evident in the 20/0600 mesoscale analysis (not shown) and the central pressure continued to fall to 978 mb. By this time the eastern portion of the storm has moved beyond the eastern edge of the ERICA observation area so that the 20/0600 January 1989 analysis was the last one completed.

H. SUMMARY OF IOP-5 DEVELOPMENT

The deepening rate considered to define an explosively deepening storm was given by Sanders and Gyakum (1980), and indicates that a storm centered at 40° latitude would need to deepen at least 17.8 mb during a 24 h period to be classified as an explosive deepening storm. The maximum deepening rate of 32 mb during the 24 period from 19/0300 to 20/0300 January 1989 exhibited by the IOP-5 storm certainly satisfies this criterion. It is therefore significant that, although the forcing is strong, the features described up to this point are not any different from those that characterize typical cyclone development.

While examining the synoptic forcing that influenced the development of the IOP-5 storm the NMC Final gridded data was used to construct plots of the 1000/500 mb thickness and the 1000 and 500 mb heights. These plots show the classic pattern of

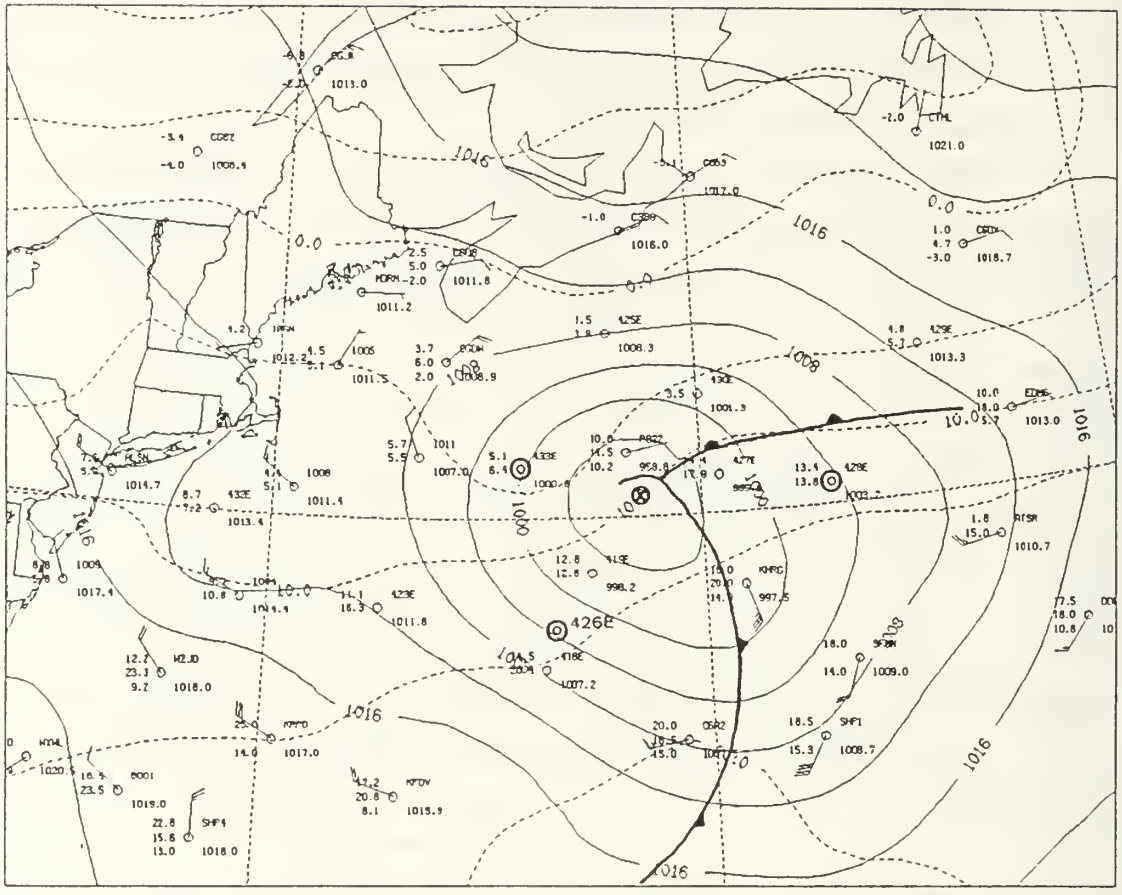

Fig. 8. IOP-5 Mesoscale Surface Analysis for 19/1800 January 1989: Same as for Fig. 4.

"self-development" described by Palmén and Newton (1969, p.326). Only the plot for 20/0000 is shown in Fig. 10 but earlier plots also resemble the figures presented by Palmén and Newton. Self-development is described as the process in which the increased amplitude of the 500 mb trough corresponds to enhanced vorticity in the trough and increased upper level divergence ahead of the trough. This enhanced upper-level divergence favors stronger low-level convergence and enhanced cyclogenesis. These plots confirm, once again, that even though the IOP-5 cyclone has developed explosively it seems to follow a pattern of traditional cyclone development.

Favorable upper-level forcing was in place almost 12 h prior to the first indications that the IOP-5 surface low was developing. The 500 mb trough and associated strong vorticity maximum were in a position that would favor development of a surface low pressure area over Virginia and North Carolina. The 80 kt 300 mb jet located over South

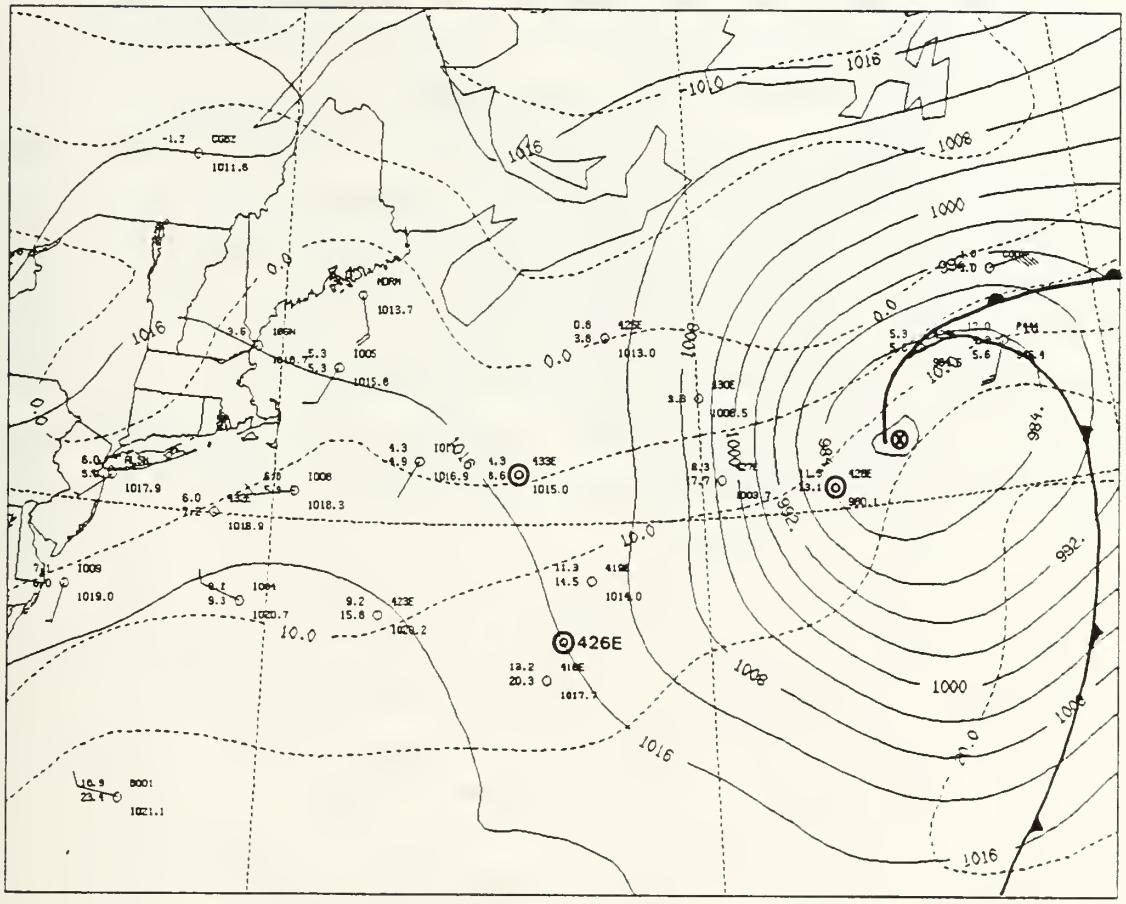

Fig. 9. IOP-5 Mesoscale Surface Analysis for 20/0300 January 1989: Same as for Fig. 4.

Carolina was also in a favorable position. The upper level forcing remained strongly favorable for cyclogenesis throughout the surface cyclogenesis period from 19/0000 to 20/0600 January, 1989.

The IOP-5 storm also developed in the region of strong sea surface temperature gradient associated with the Gulf Stream, and continued to remain within the influence of the Gulf Stream SST gradient throughout its development. Lilly (1990) noted that the IOP-2 storm also maintained a similar relationship to the Gulf Stream SST gradient. In addition, he observed that the surface air temperature thermal gradient was parallel to the Gulf Stream SST gradient and that the IOP-2 storm was generally characterized by weak warm advection. In contrast, moderate warm advection was evident east of the the developing IOP-5 low center even in the early stages of development, and warm advection increased in strength as the storm developed. North of the IOP-5 warm front,

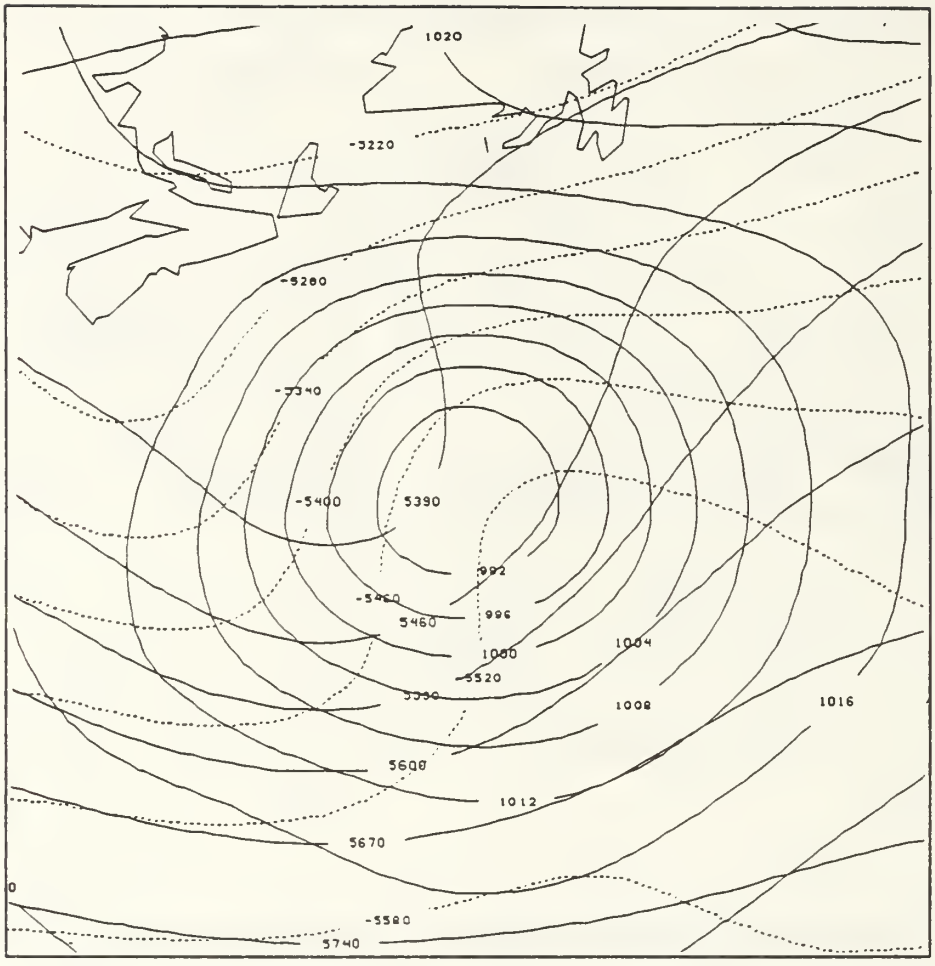

Fig. 10. NMC Final 1000/500 mb Heights and Thickness 20/0000 January 1989: Units for height are m. Dashed lines represent 1000:500 mb thickness.

the flow pattern was similar to that described by Lilly (1990) for the IOP-2 storm, such that winds were largely parallel to the thermal gradient. Lilly (1990) also noted that the surface air temperature increased rapidly east and northeast of the IOP-2 low and that air-sea temperature differences were large. These observations were based largely upon analyses of buoy air and sea temperature observations. He suggested that cold outflow from the preexisting storm to the southeast, combined with weak surface warm advection and rapid rises in the surface air temperature, implied that surface heat fluxes must be playing a role in the development of the IOP-2 cyclone.

Although large rises in surface air temperature were not observed during the IOP-5 storm there was still evidence that that surface heat fluxes were important. In the region north of the warm front the easterly surface winds are generally parallel to the thermal gradient indicating only weak thermal advection; however, the surface air temperatures are warmer than would be expected within this region. The analysis of the pattern of buoy air-sea temperature differences presented in the next chapter confirms that the air north of the surface warm front is indeed warmer than would be expected in this region of weak thermal advection. This lack of warm advection suggests that another heat source, such as the positive heat fluxes that occur north of the warm front, is causing an increase in the surface air temperatures. This unusual characteristic, common to both IOP-2 and IOP-5, may be a significant factor in the explosive development of these storms.

V. BOUNDARY LAYER FORCING

The synoptic discussion in the previous chapter established that upper-level forcing was favorable for the initial development of the IOP-5 storm and remained favorable throughout its development. Furthermore, development of the IOP-5 cyclone appeared to follow a pattern of typical cyclone development, even though the storm deepened explosively. In order to isolate the features that distinguish the IOP-5 storm from a typical nonexplosive deepening storm, the mesoscale analyses were used to examine the surface processes of the IOP-5 storm and their roles in the boundary layer forcing that contributed to explosive cyclogenesis. This chapter includes several sections that examine the various aspects of the boundary layer forcing. The first section evaluates the surface thermal advection and its contributions to modification of the surface thermal gradient. The vertical structure of the thermal advection will be examined as well to determine the role of surface advection in relation to advection in the layers above the surface. The second section describes the pattern of surface sensible heat fluxes associated with the IOP-5 storm and examines their contribution to the stability of the boundary layer and convective procceses. The third section evaluates the significance of the air-sea temperature differences in relation to the thermal forcing associated with the IOP-5 storm, while the final section examines the potential for coupling surface processes to the upper atmosphere in a moist symmetrically neutral environment.

A. THERMAL ADVECTION

The discussion of the surface flow patterns contained in the previous chapter provided qualitative evidence that moderate warm advection east of the low was present even in the early stages of development. The strongest warm advection was associated with the region just south of the warm front, while immediately north of the warm front the winds were easterly and parallel to the strongest thermal gradient associated with the warm front. The strong northerly winds west of the cold front supported cold advection but it was not until the later stages of development that the cold advection was sufficiently strong to overcome the influence of the Gulf Stream and form a strong thermal gradient along the cold front.

The surface thermal advection is examined using the Brown-Liu boundary layer model generated winds and the mesoscale thermal analyses to assess the amplification of the thermal perturbation due to low-level warm and cold advection. The surface

thermal advection is plotted in units of ° K day^{-1} . At 18/2100 (Fig. 11), when the surface low pressure center has yet to appear, there was a region of warm advection east of where the low forms and a region of cold advection to the west. The size and magnitude of the regions of cold and warm advection were similar at this stage with a maximum of 30° K day^{-1} for both. This thermal advection pattern supports initial low level cyclogenesis. By 19/0600 (Fig. 12) a large region of warm advection is present along and north of the warm front to the east of the surface low. This advection is characteristic of a developing low, although the average warm advection rate of 10° K day^{-1} is substantially less than the cold advection rate of 50° K day^{-1} west of the low. Since surface winds in the warm sector are strong and southerly, some other feature of the atmospheric forcing may be acting to reduce the degree of warm advection in this region.

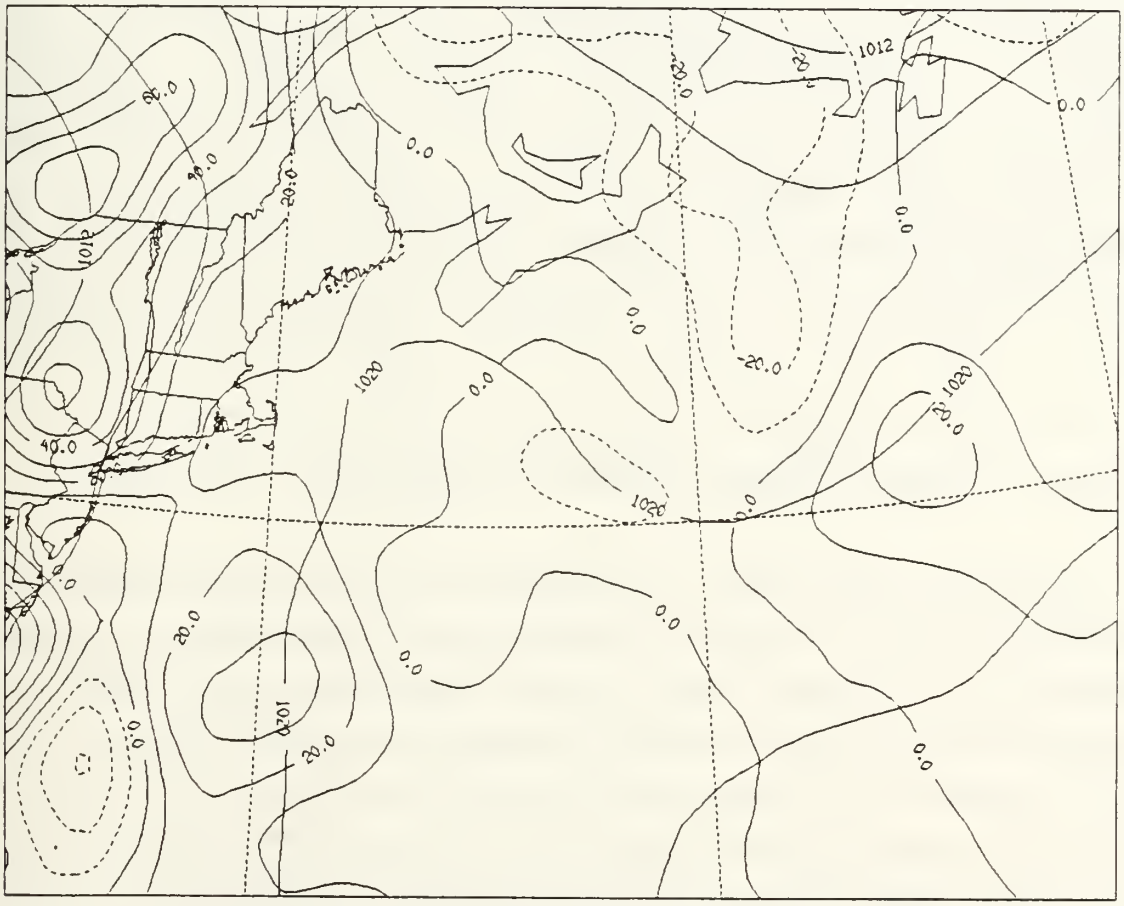

Fig. 11. Thermal Advection at 18/2100 UTC January 1989: Thermal advection was calculated using the IOP-5 mesoscale thermal analyses and the Brown-Liu PBL model winds. Solid lines represent warm advection and dashed lines represent cold advection at 10° K day^{-1} interval.

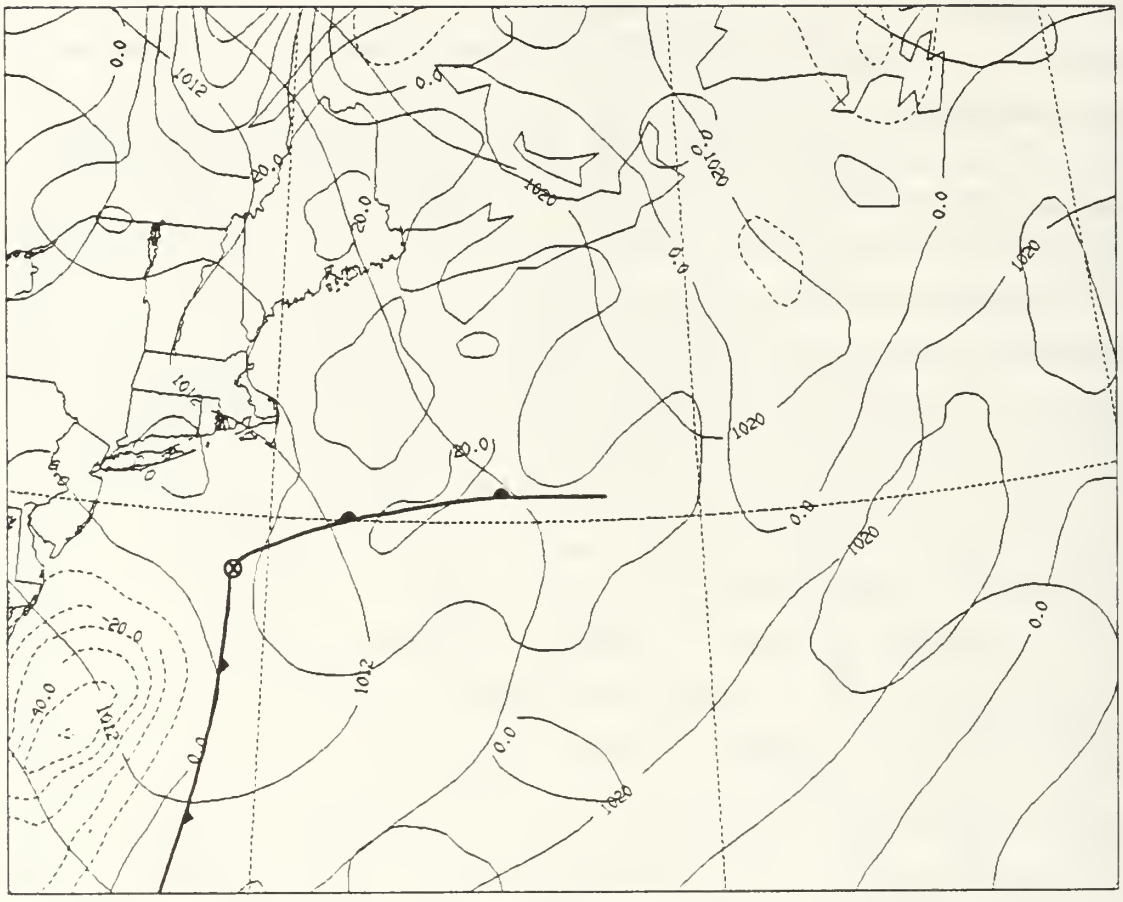

Fig. 12. Thermal Advection at 19/0600 UTC January 1989: Same as Fig. 11

Neiman et al. (1990) suggest that the boundary layer could become decoupled from the layer just above it, resulting in strong advection in the upper layer and weak advection in the boundary layer. This result required very stable boundary layer stratification that was caused by warm air flowing over colder water. Subsequent analysis of the fluxes for IOP-5 suggest that this did not occur in this case. To examine the possibility that much stronger thermal advection occurred just above the boundary layer of the IOP-5 storm, the 12 hourly NMC gridded data from the Global Data Assimilation System (GDAS) were used to calculate temperature advection fields at both 1000 and 850 mb. This data has a grid resolution of 2.5°, compared to the finer resolution (20 km) of the data set used to calculate the IOP-5 thermal advection, and tends to produce reduced values of thermal advection. The 1000 mb thermal advection at 19/1200

(Fig. 13) shows the maximum cold advection west of the cold front to be approximately 30° K day^{-1} and the warm advection into the warm sector and ahead of the warm front to be much weaker at 20° K day^{-1}. The magnitude and distribution of the thermal advection in the NMC analysis is comparable to that calculated from the PBL model winds and mesoscale thermal analyses, which provides some confidence in the computation and its use for comparison with the thermal advection in Fig. 12. The 850 mb (1500 m) thermal advection for the same time (Fig. 13) showed substantially stronger warm advection with a maximum rate of 30° K day^{-1}, comparable in area and magnitude to the cold advection west of the cold front. Although this suggests some decoupling in the PBL is possible, by 20 0000 both the 1000 mb thermal advection and 850 mb thermal advection (Fig. 14) show comparable magnitudes of cold and warm advection at both levels. The intensity of the cold advection has increased to 90° K day^{-1}, indicating intensification of the cyclone. This analysis could indicate that conditions within the boundary layer were different from those in the layer above, but it is more likely that the weaker warm advection near the surface is due to the stronger influence of surface friction on the circulation within the warm sector. Other factors that could reduce the surface warm advection are weakening of the southerly flow due to a preexisting circulation to the north, or vertical transport of heat away from the surface that reduces the heat available for horizontal advection.

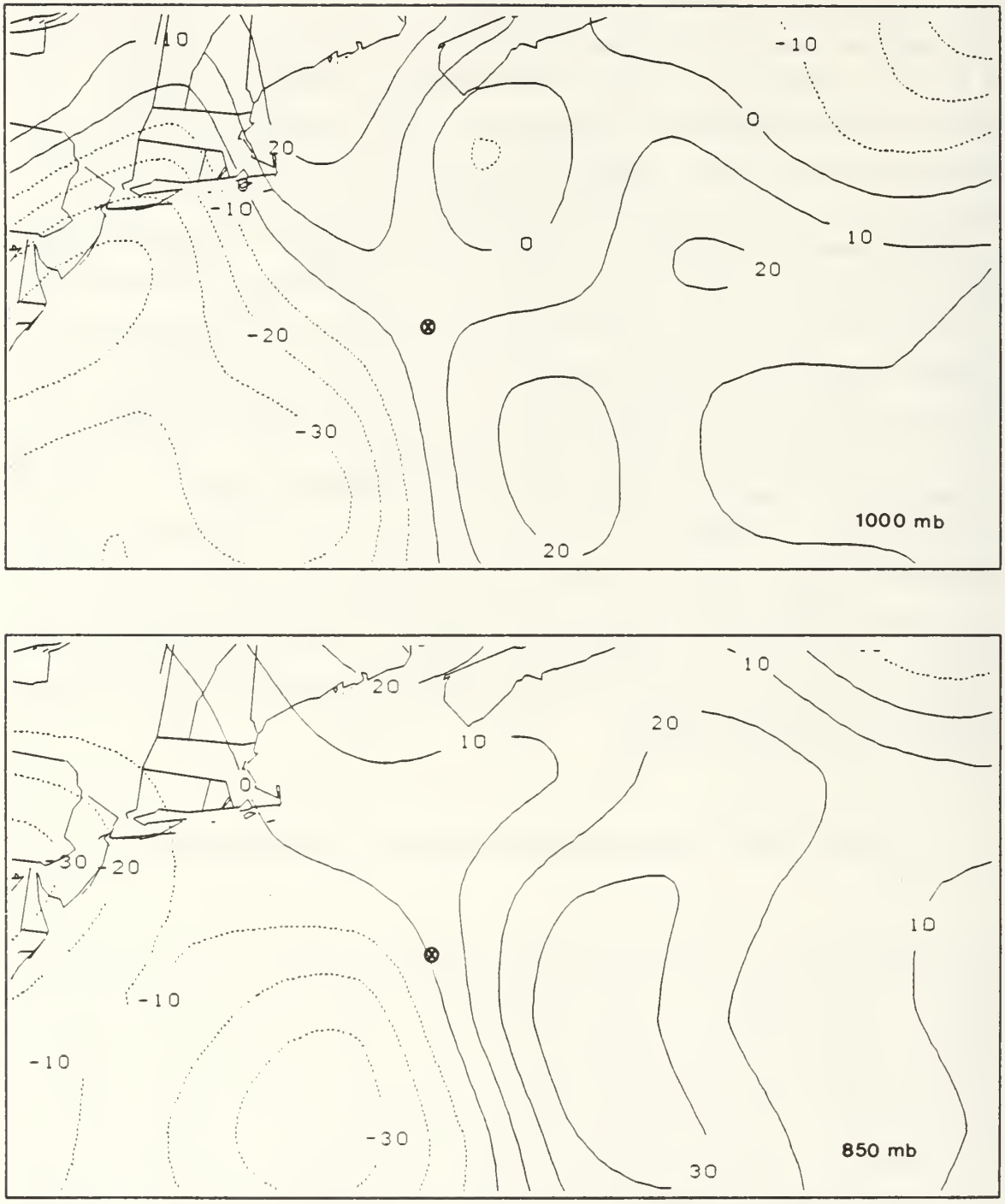

Fig. 13. NMC Thermal Advection at 19/1200 UTC January 1989: Warm advection (solid) cold advection (dashed) at 10° K day^{-1} contour interval.

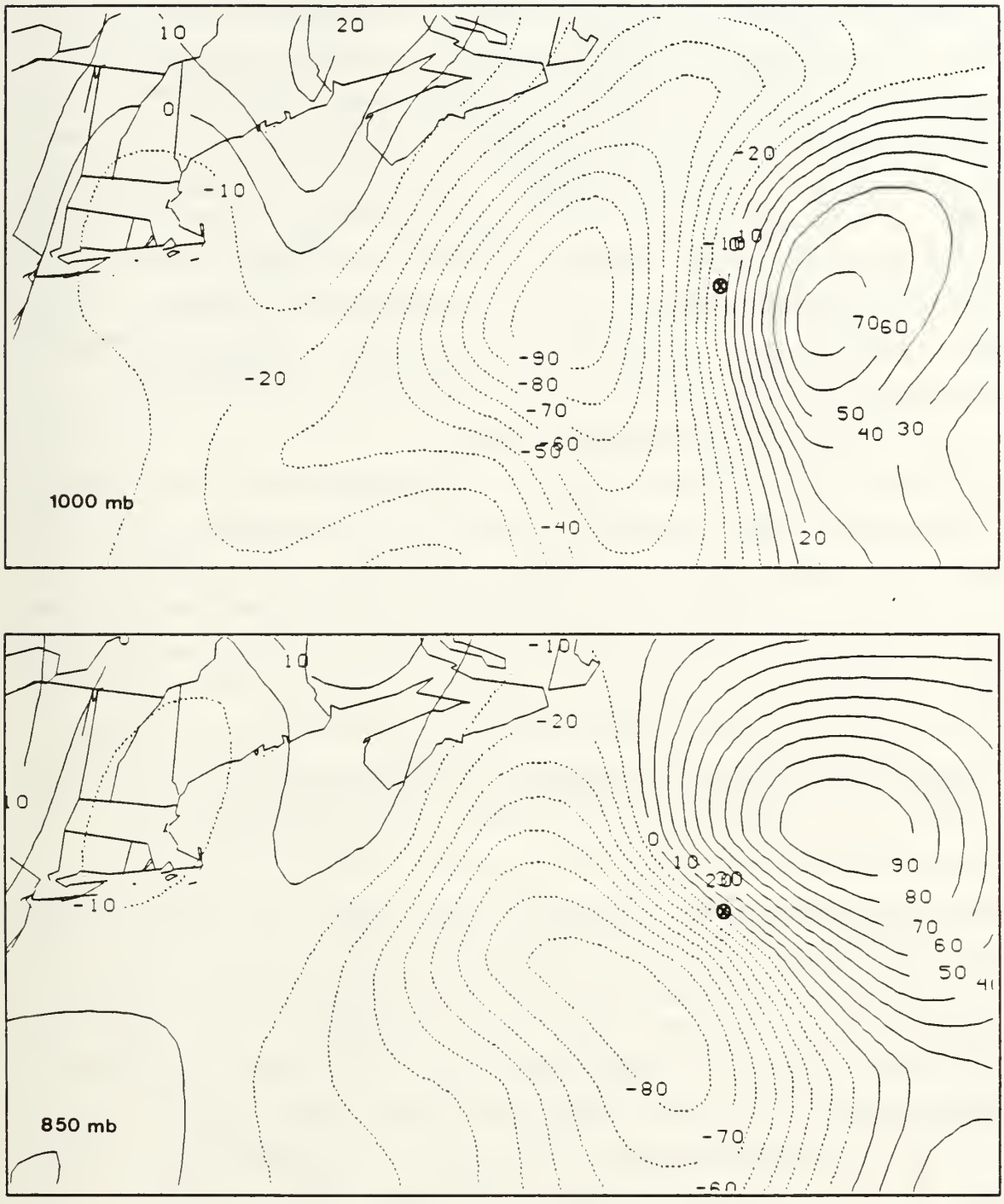

Fig. 14. **NMC Thermal Advection at 20/0000 UTC January 1989:** Same as Fig. 13.

The preceding analysis confirms that significant warm advection is occurring at the surface as well as just above the PBL throughout the development of the IOP-5 storm. In spite of this strong warm advection, the isotherms along the warm front do not move significantly northward and their gradient only strengthens slightly as the storm develops, which suggests that air-sea interaction with the Gulf Stream and associated boundary layer processes act to maintain this structure. These processes are explored more fully in the next section. Moreover, the surface air temperatures within the warm sector increased very little with time which is inconsistent with the amount of warm advection taking place. It is likely that the heat is being transported away from the boundary layer, which may contribute to latent heat release and convection.

B. ANALYSIS OF SENSIBLE HEAT FLUXES

To characterize the surface interaction and the contribution of the surface fluxes to low level thermal evolution, the sensible heat flux and wind stress patterns of the IOP-5 cyclone were calculated using the Brown-Liu boundary layer model. As discussed earlier, the latent heat fluxes were not calculated since sufficient numbers of reliable dewpoint temperature observations were not available and thus, the present discussion ignores the moisture flux contribution to cyclogenesis. Prior to development of the IOP-5 low pressure center, the heat flux distribution at 18/1800 (Fig. 15) demonstrates the influence of the Gulf Stream SST gradient on the surface flux pattern. Positive fluxes of 100-150 W m^{-2} characterize the entire region south of the northern edge of the strongest Gulf Stream SST gradient (Fig. 6), and zero or negative fluxes characterize the region north of this gradient. The presence of positive heat fluxes south of the Gulf Stream indicates that the surface air temperatures are cooler than the underlying sea surface temperatures. The source of the cooler air that produces this flux pattern is probably the preexisting cyclone to the north over Newfoundland (Fig. 15) and the associated weak cold advection behind its cold front. The geostrophic flow around this low supports weak cold surface advection over the Gulf of Maine and Gulf Stream regions, which presumably forced cooler air southward across the Gulf Stream and generated the positive heat fluxes that characterize the region of incipient IOP-5 development. The existence of these positive fluxes prior to development of the IOP-5 low suggests that the atmosphere is being preconditioned by enhanced warming and moistening prior to cyclogenesis.

By 18/2100 the surface heat fluxes over the ocean just east of Virginia, where the low will develop, have increased to a maximum of 200-250 W m^{-2} (Fig. 16). The low sub-

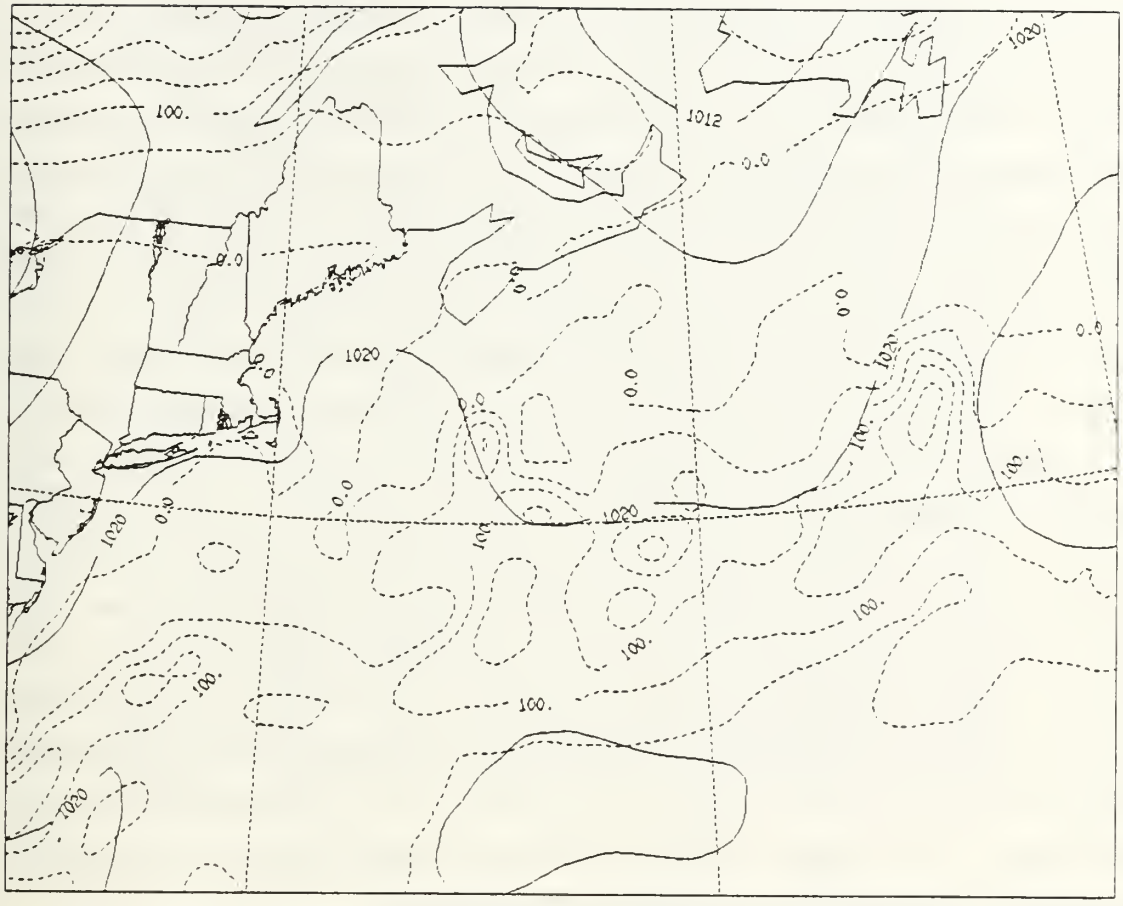

Fig. 15. Sensible Surface Heat Fluxes at 18/1800 UTC January 1989: Contour interval is 50 W m^{-2}.

sequently develops in this region of increased heat flux, which is also characterized by surface cold advection as seen in the previous section. The weak northerly cold advection associated with the preexisting low probably reduced the amount of surface heating expected to result from the strong positive heat fluxes. By 19/0000 the mesoscale analysis (not shown) shows weak 5-10 kt southerly surface winds south and north of the region where the IOP-5 storm will develop. This suggests that the cold advection associated with the preexisting storm to the northeast is no longer a strong influence on the circulation in this region. Still, the weaker warm advection associated with the early stages of the IOP-5 storm may have resulted, in part, due to the offsetting effect of cold advection from the north.

At 19/0000 the surface low pressure area has developed, and strong positive heat fluxes of 350 W m^{-2} occur west of the developing low and moderate positive heat fluxes

of 150 W m^{-2} occur east of the low (Fig. 17). GOES IR imagery for 19/0001 (Fig. 18) indicates a region of convective clouds is positioned directly above the heat flux maximum east of the developing low, which suggests that the heat is being transported upwards through a deep vertical layer. The next 9 h are characterized by a similar pattern, with the intensity of the surface heat fluxes increasing slightly and some expansion of the area of positive fluxes west of the low. The surface heat flux analysis at 19/0900 (Fig. 19) shows this evolution and indicates a substantial region in the warm sector where the heat flux maximum exceeds 200 W m^{-2}. Interestingly, this increase in the strength of the surface heat flux in the warm sector has occurred in a region characterized by surface warm advection. Evidently, the convection noted above resulted in either significant adiabatic cooling or mixing of cooler air down into the boundary layer that reduced the amount of surface heating. This pattern of positive fluxes to the southeast and slightly north of the warm front continues through the period of most rapid cyclogenesis as shown by the heat flux analysis for 19/1500 (Fig. 20). The fluxes within the warm sector remain fairly constant as shown by the 19/1800 heat flux analysis (Fig. 21), although a decrease in the magnitude of the positive fluxes is expected because increased warm advection has resulted in a reduction in the air-sea temperature difference. Evidently, the stronger circulation is helping to maintain relatively large fluxes in the presence of decreasing air-sea temperature differences.

By 19/2100 the substantially reduced but still positive fluxes in the warm sector (Fig. 22) suggest that this reduction in air-sea temperature difference has occurred. This is confirmed by the air-sea temperature difference plot at 19/2100 (Fig. 23), where the air-sea temperature difference is near zero in this region. Fig. 23 also shows that even though the IOP-5 storm is well-developed, the pattern of air-sea temperature differences continues to be strongly influenced by the Gulf Stream SST gradient shown in Fig. 6. By 20/0300 the air-sea temperature difference analysis (Fig. 24) shows continued strong warm advection has raised the air temperature east of the low center, causing the air temperature to be 4° C warmer than the sea temperature. This region corresponds to an area of zero and possibly small negative fluxes east of the low shown on the heat flux plot for 20/0300 (Fig. 25). To the west of the low center is a darkened bull's-eye region in the heat flux pattern that indicates that the the PBL model failed to converge to a solution as a result of the large air-sea temperature differences and very strong geostrophic winds generated by the strong pressure gradient in this area. Although the flux values for this region are not reliable, they do not influence the solution elsewhere

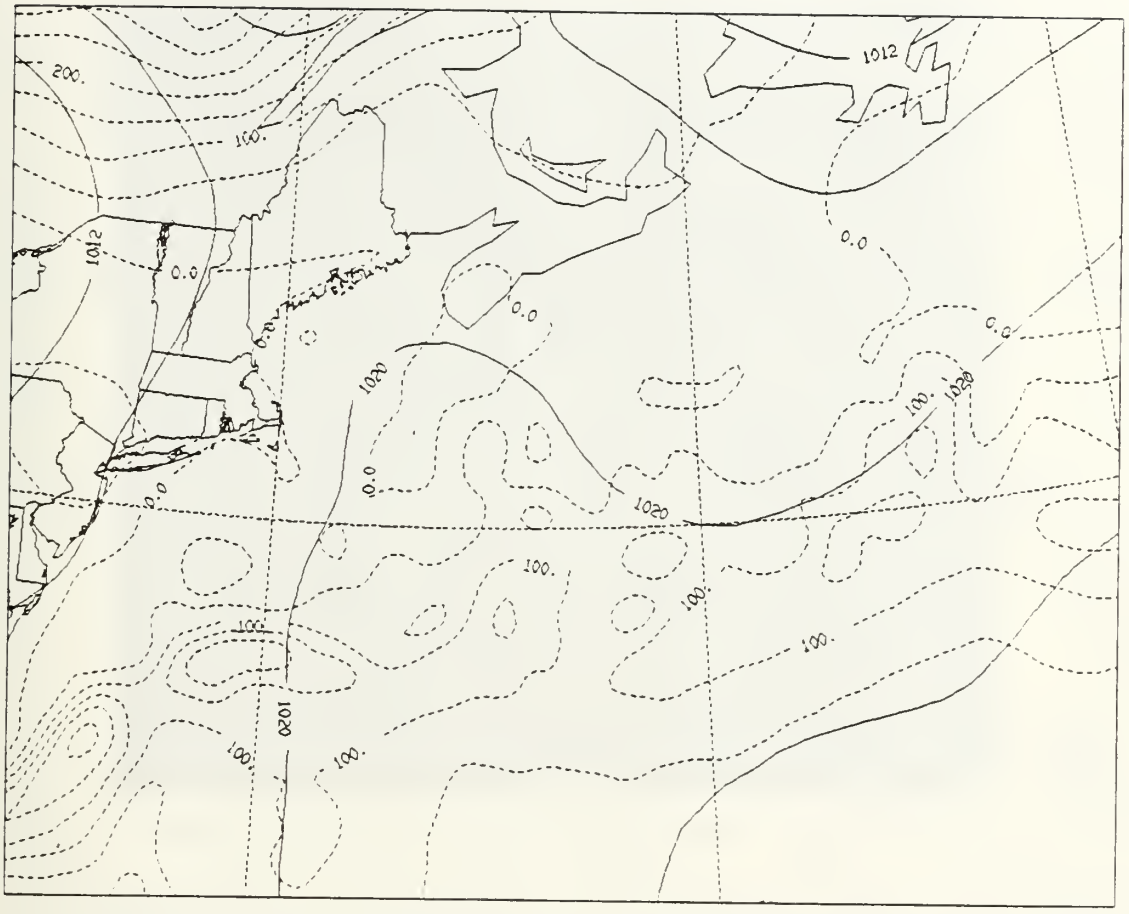

Fig. 16. Sensible Surface Heat Fluxes at 18/2100 UTC January 1989: Same as Fig. 15.

in the domain. This was the latest time analyzed since by 20/0600 the eastern half of the IOP-5 storm had moved beyond the eastern edge of the observation area.

Examination of the pattern of surface heat fluxes associated with the developing IOP-5 low shows that the region of positive fluxes east of the low extends northward across the warm front. Therefore, the surface heating associated with the fluxes tends to strengthen the thermal gradient north of the warm front rather than along the warm front itself. Considering only the thermal gradient when conducting the mesoscale analyses of IOP-5 would have resulted in positioning the warm front further north to coincide with the northern edge of the strongest thermal gradient. Instead, the analyses place the warm front further south to be consistent with the surface wind observations that clearly show wind shifts characteristic of those across a front. It should also be noted that the pattern of positive heat fluxes and surface heating is strongly influenced by the

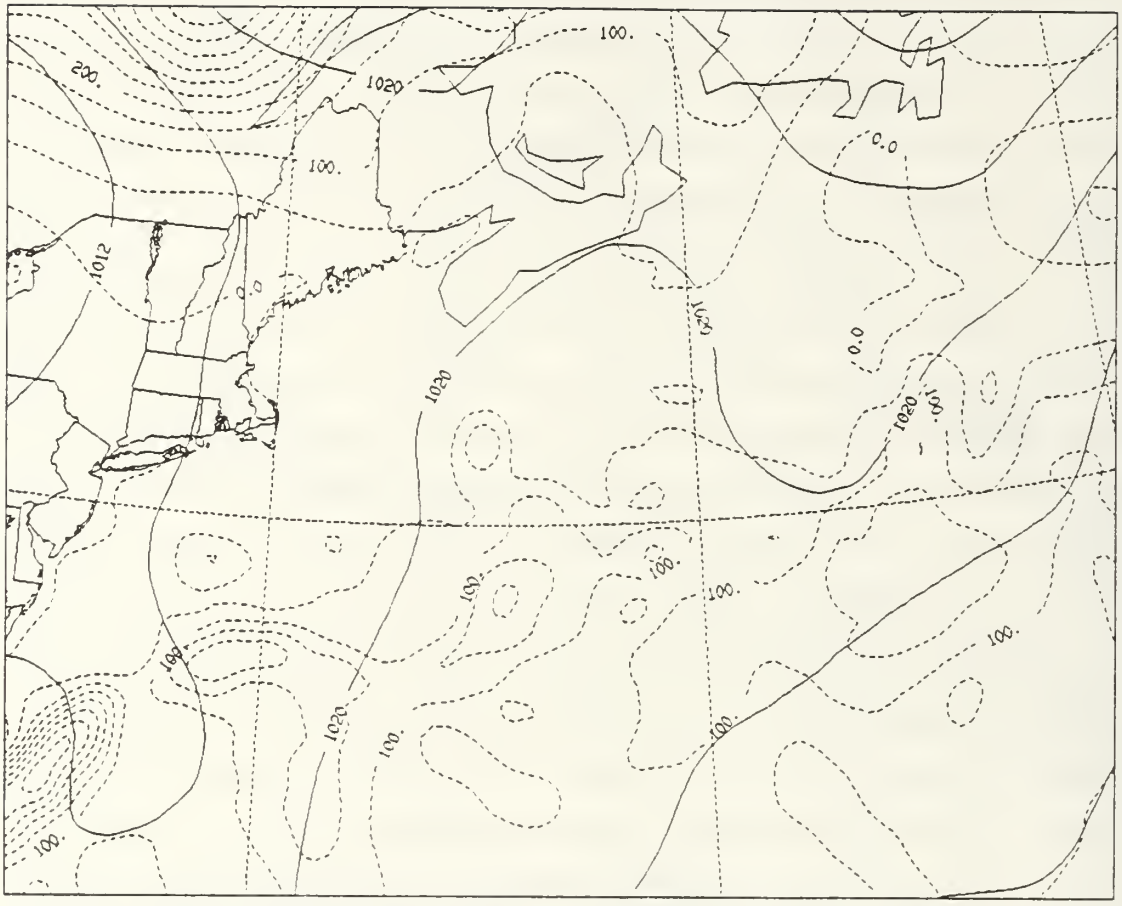

Fig. 17. Sensible Surface Heat Fluxes at 19/0000 UTC January 1989: Same as Fig. 15.

ocean mesoscale features, such as the Gulf Stream eddies, and may be influenced by the mesoscale structure of the atmosphere as well. These features may have modified the position of the thermal gradient that would normally have resulted from the actions of the storm circulation and associated warm advection.

The location of positive fluxes throughout the region east of the low and extending just across the warm front to the north significantly affected the stability within the warm frontal region. Surface heating that results from this heat flux pattern would destabilize the upglide region associated with the warm front, as well as the region south of the warm front, and stabilize the atmosphere north of the warm front (where the fluxes are zero or negative). Lilly (1990) observed similar heat flux patterns associated with the IOP-2 storm. These conditions, observed for both the IOP-5 and IOP-2 storms, differ significantly from the conditions observed in the idealized model study conducted

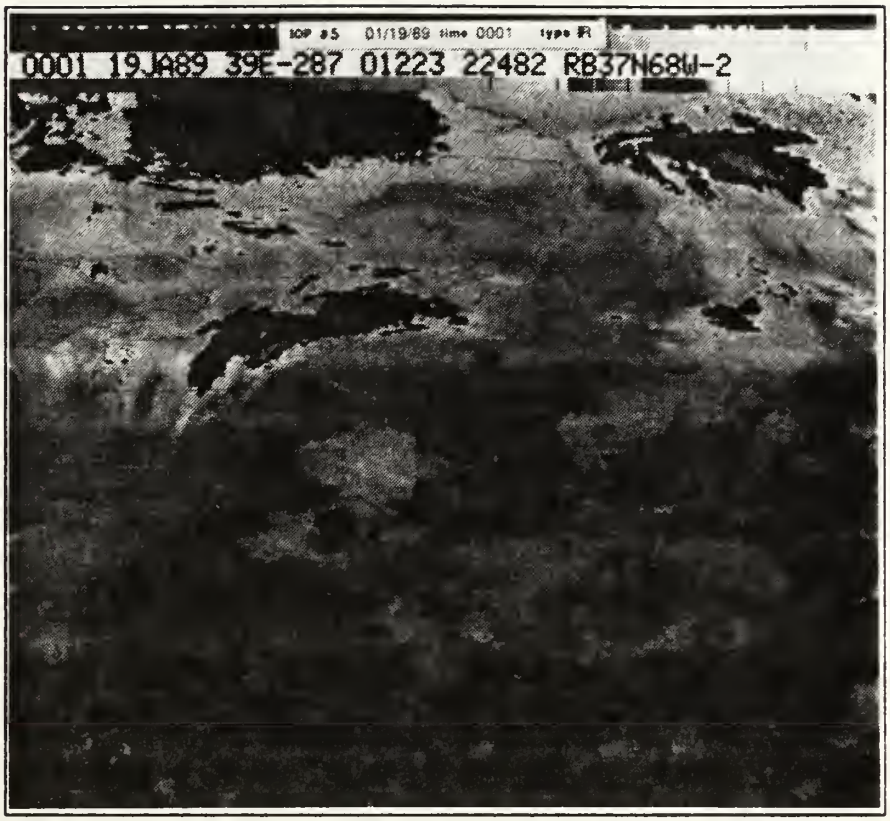

Fig. 18. GOES IR Imagery for 19/0001 January 1989: Same as Fig. 2.

by Nuss (1989), where the fluxes were positive north of the warm front, small or negative along the warm front itself, and negative within the warm sector south of the warm front. Nuss (1989) suggested that this pattern of heat fluxes resulted in surface heating that caused unstable stratification of the atmosphere to the northeast of the warm front and stable stratification along and just south of the warm front, leading to enhanced vertical circulation through enhanced frictional convergence in the PBL. In order to assess the amount of frictional convergence associated with the IOP-5 storm the Brown-Liu boundary layer model was used to calculate the surface wind stress and the curl of the wind stress. Unfortunately, the model's point by point evaluation of the atmospheric stability failed to capture the continuous nature of the atmosphere and resulted in small scale structure in the fields that may have masked the larger scale features. Furthermore, the mesoscale structure of the real atmosphere of the IOP-5 storm makes analysis of PBL stability much more difficult than analysis of the idealized atmosphere completed during the model study by Nuss (1989).

Up to this point, this discussion has focused on the positive fluxes east of the IOP-5 low, but the effect of the large positive fluxes west of the low should also be examined. The surface heat flux plots show that the positive fluxes in this region strengthen considerably as the storm develops. This feature is consistent with the increased temperature differential that results from the enhanced cold advection associated with the increased circulation. Even though these fluxes are strong, they occur within the subsidence region of the storm, and are not as dynamically significant as the the positive fluxes that occur to the east of the storm.

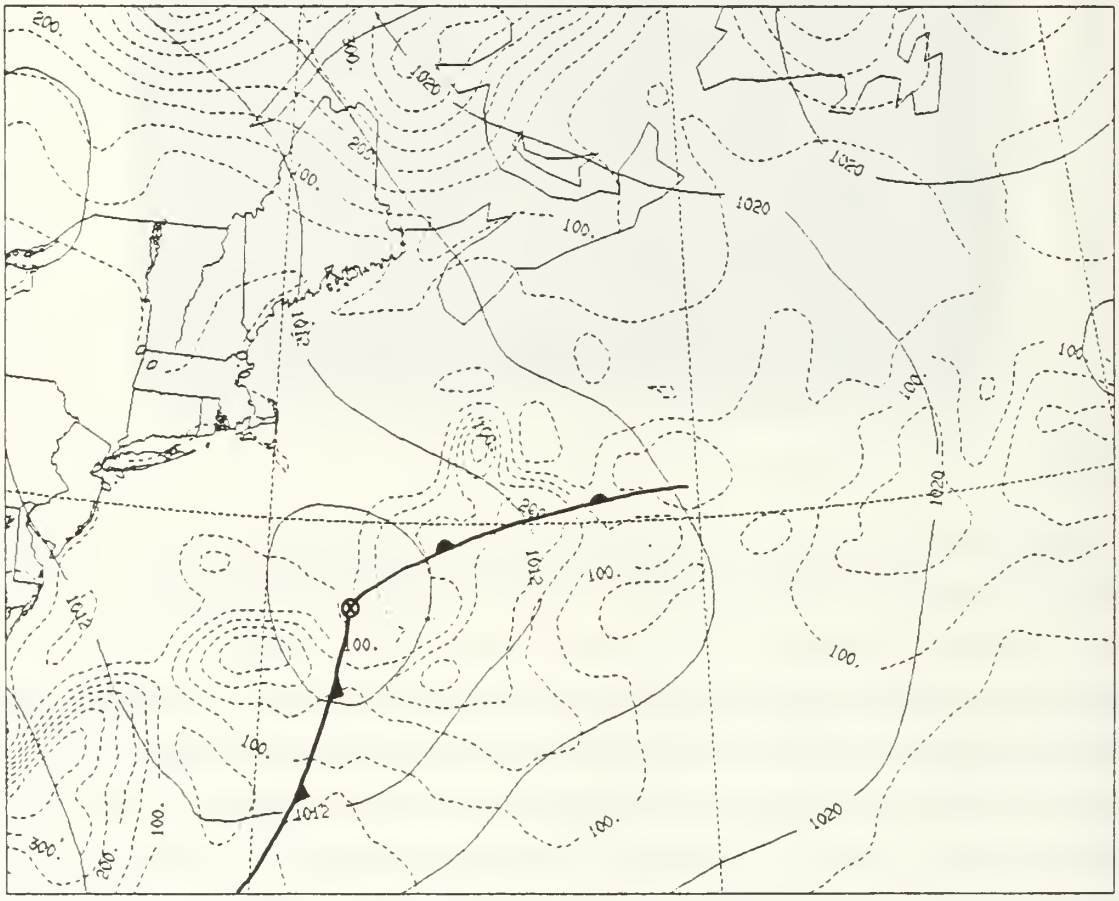

Fig. 19. Sensible Surface Heat Fluxes at 19/0900 UTC January 1989: Same as Fig. 15.

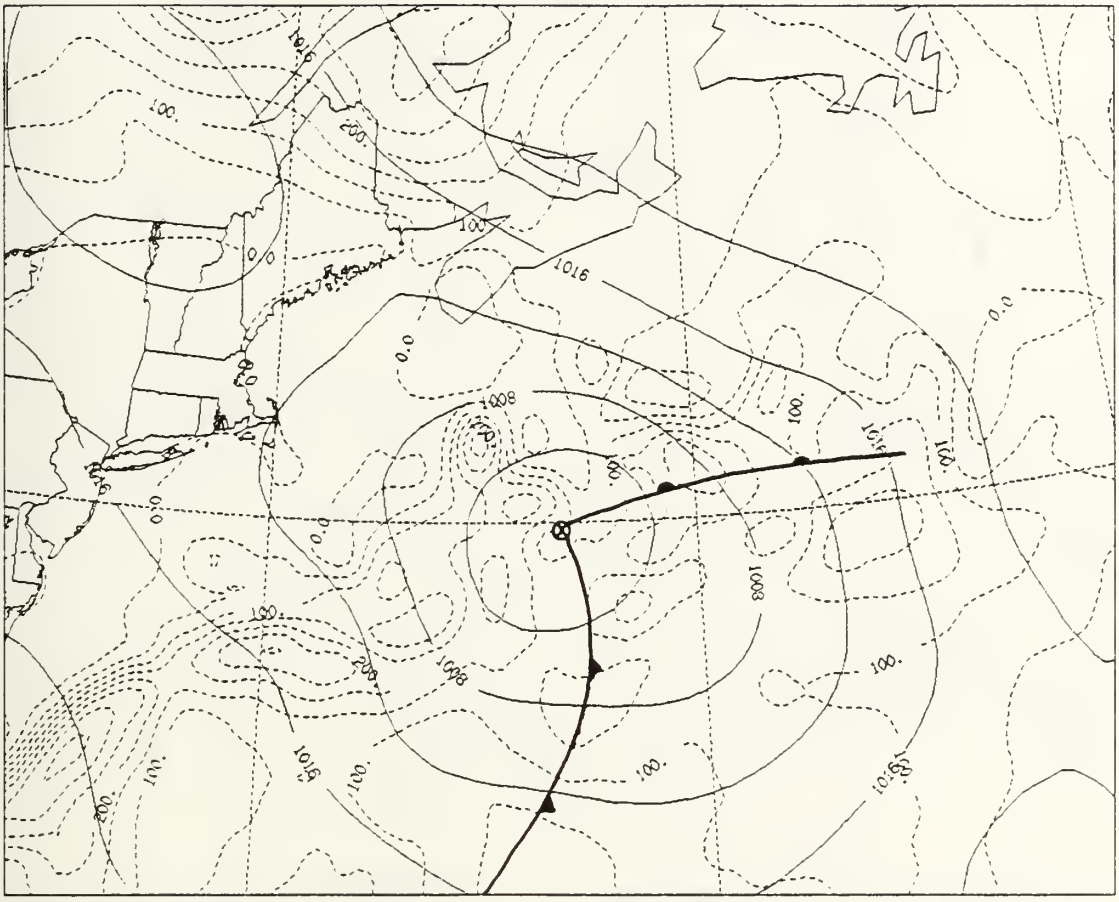

Fig. 20. Sensible Surface Heat Fluxes at 19/1500 UTC January 1989: Same as Fig. 15.

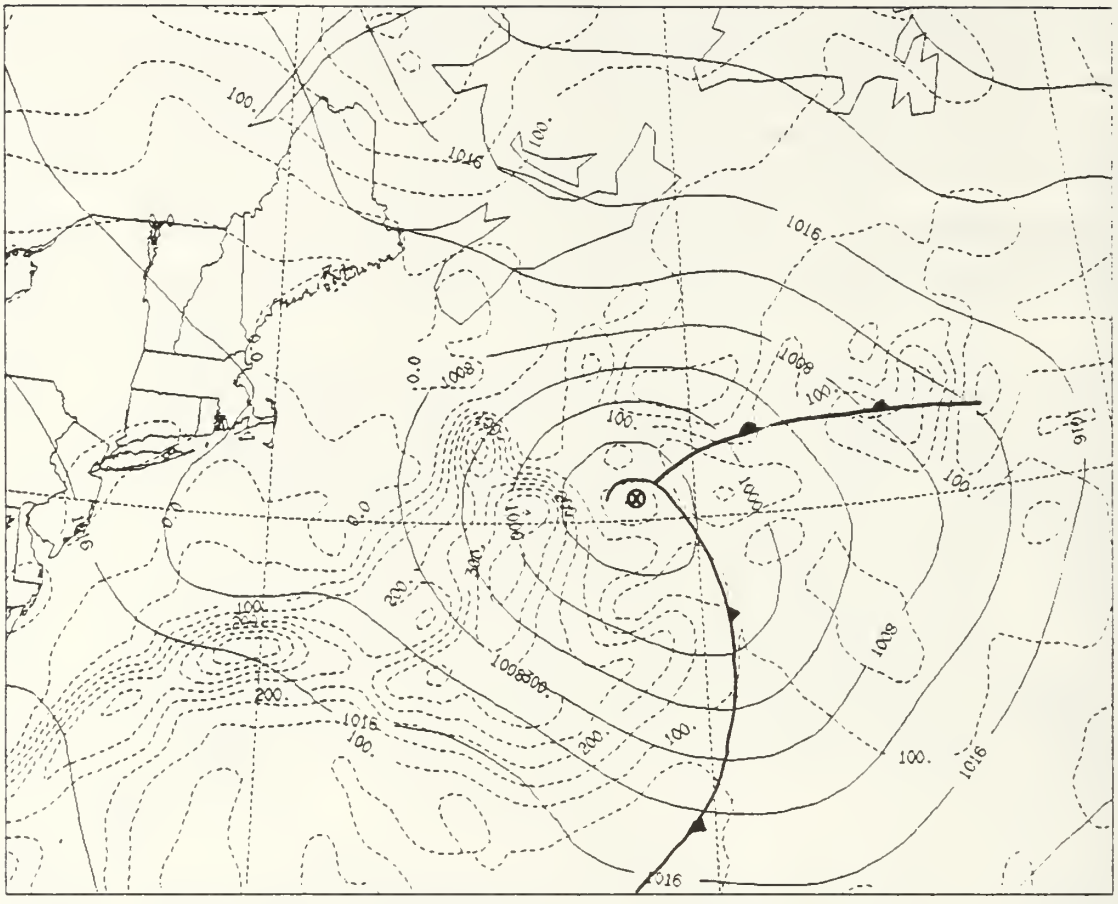

Fig. 21. Sensible Surface Heat Fluxes at 19/1800 UTC January 1989: Same as Fig. 15.

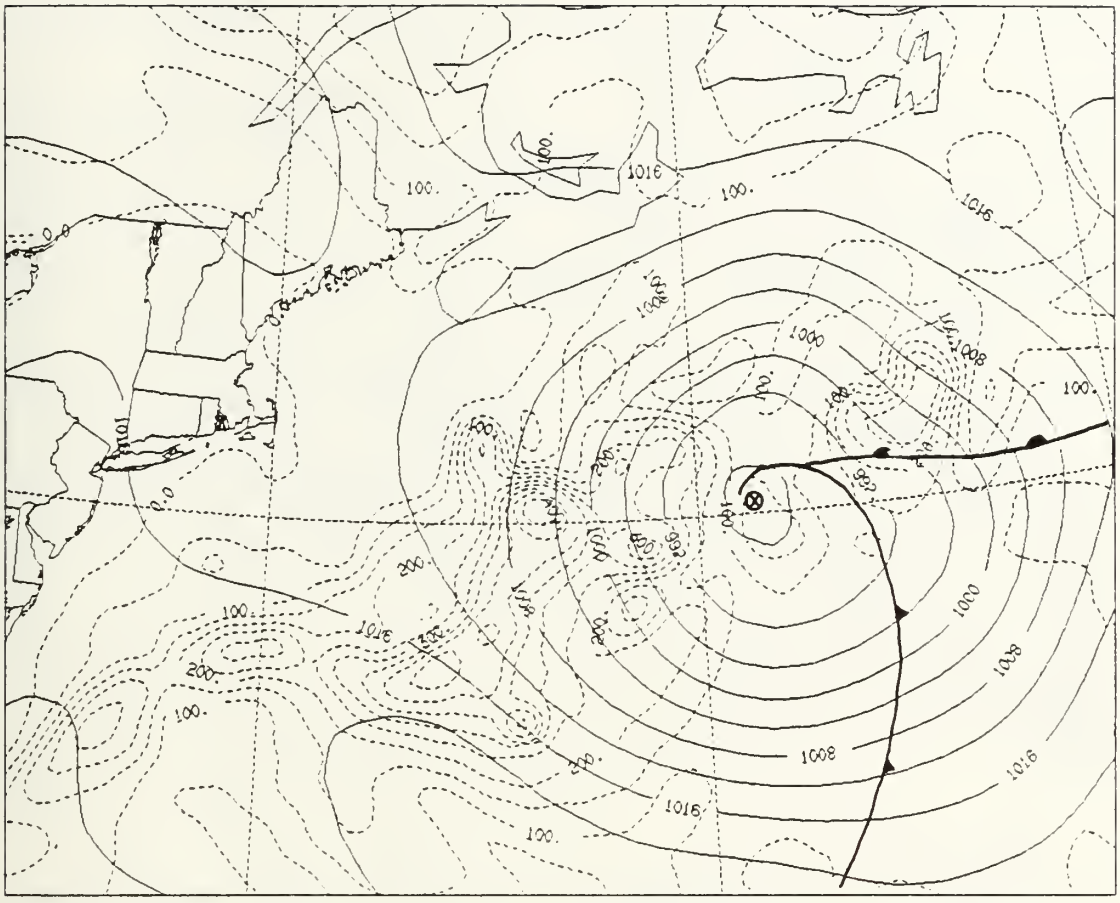

Fig. 22. Sensible Surface Heat Fluxes at 19/2100 UTC January 1989: Same as Fig. 15.

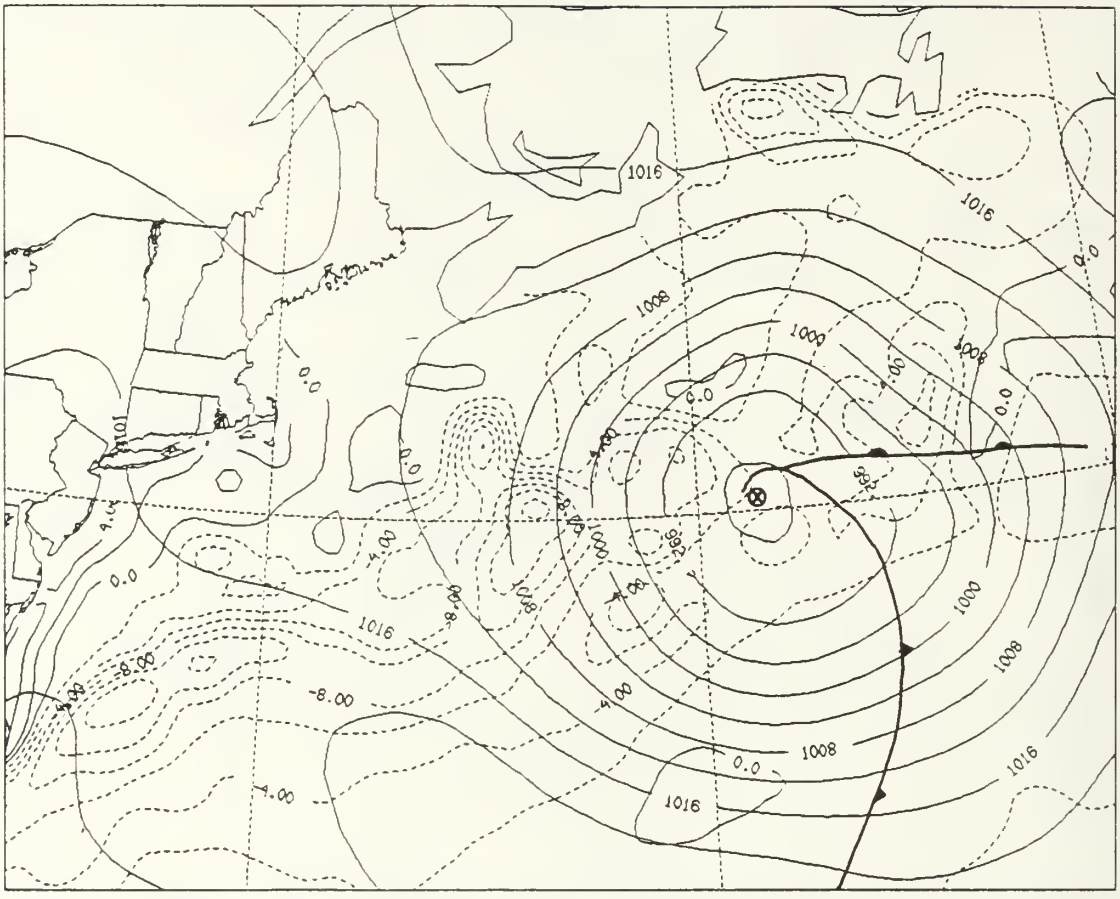

Fig. 23. Air-Sea Temperature Differences at 19/2100 UTC January 1989: Contour interval is 2° C. Negative values indicate sea temperature is warmer than air temperature.

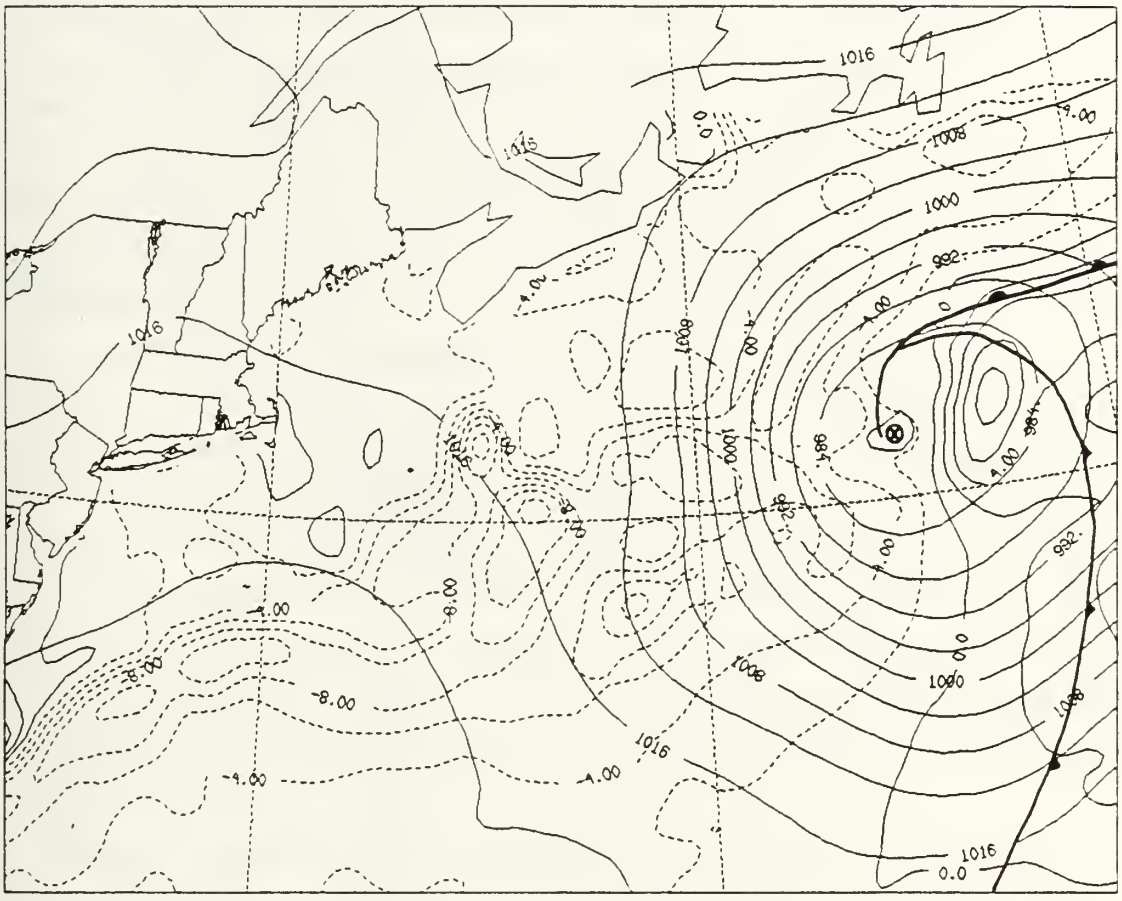
1016
1016
1016
1016
1008
1000
992
984
1000
1008
1016
1016
0.0
-4.00
-8.00
-8.00
-4.00
-4.00
-8.00
-4.00
-4.00
-8.00
-4.00
-4

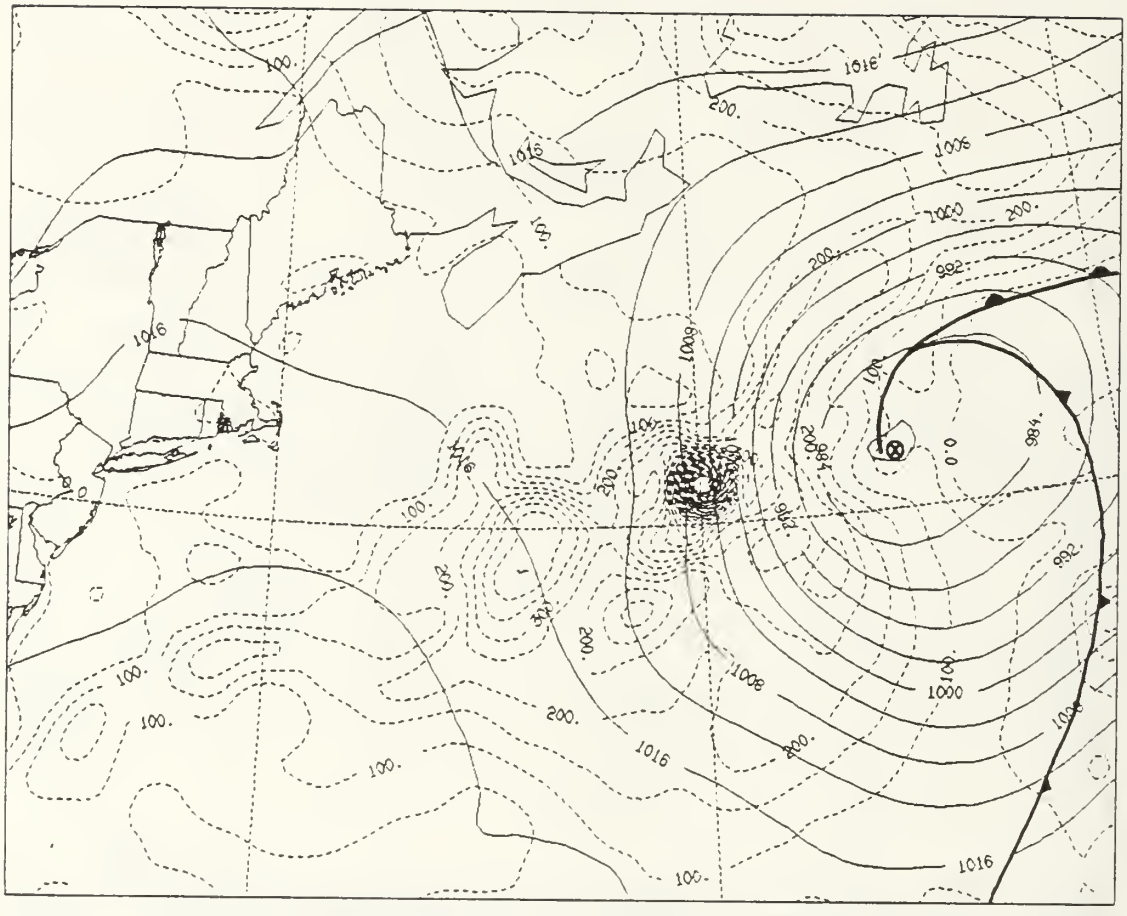

Fig. 25. Sensible Surface Heat Fluxes at 20/0300 UTC January 1989: Same as Fig. 15.

As noted previously, there is a lack of surface layer warming in regions where both warm advection and positive surface heat fluxes are occurring, which indicates that heat is being transported away from the surface. To crudely estimate the vertical heat transport within the warm sector, the terms in a modified form of the thermodynamic energy equation were estimated from the other available analyses. The thermodynamic energy equation is

$$\frac{\partial T}{\partial t} = -\vec{v}\nabla T + F_h - \omega\left(\frac{\partial T}{\partial p} - \frac{\alpha}{C_p}\right).$$

The first term represents the local change in air temperature at the surface. The local change was estimated by differencing the 3 hourly analyses, and was found to be ap-

proximately 1° C day^{-1} in the warm sector. The second term represents the thermal advection (in this case the warm advection within the warm sector), and an estimated average value for warm advection of 15° C day^{-1} was obtained from the thermal advection analyses presented in Section A. The third term represents the contribution by the sensible heat flux divergence. Following Lilly (1990), an estimate of 0.9° C per 3 h period is obtained assuming a flux of 100 W m^{-2} is distributed over a 1 km deep boundary layer. Applying this estimate to the average flux of 150 W m^{-2} in the warm sector of the IOP-5 storm (estimated from the heat flux plots) results in an estimate of 11° C day^{-1} for the third term. Since the vertical mixing of the heat fluxes may be over a substantially deeper layer than 1 km, this estimate gives an upper bound on the posssible boundary layer warming. Substituting these values into the previous equation, a value of -25° C day^{-1} is obtained for the fourth term, which represents the combined effects of the vertical advection and the adiabatic processes that result in the vertical transport of heat in the atmosphere. Based on a moist adiabatic lapse rate and a rough estimate of the adiabatic expansion rate, the vertical transport of thermal energy would be approximately -8 $\mu b\ s^{-1}$, which equates to 8 cm s^{-1}, and suggests a substantial amount of upward vertical motion within the warm sector of the IOP-5 storm.

C. AIR-SEA TEMPERATURE DIFFERENCE EVOLUTION AT SELECTED BUOYS

As indicated by the surface isotherm analyses in the last chapter, the low-level thermal pattern changes very little as the storm passes. This was confirmed by the very similar patterns of surface heat flux and air-sea temperature differences noted in the previous section. To further support this pattern of air-sea interaction, the actual air-sea temperature differences at several different locations with respect to the IOP-5 storm track were examined. Observations collected at three of the ERICA drifting buoys were used to generate plots of the air-sea temperature difference (ΔT) versus time (Fig. 26) as well as three tables listing the 3 hourly air and sea temperature observations (Tables 3, 4 and 5). Since the air-sea temperature differences are strongly influenced by the SST gradient, it is necessary to look at the actual air and sea temperature observations to determine whether a change in the ΔT indicates a change in sea temperature or a change in air temperature.

Buoy 426E was located south of the path of the IOP-5 storm at approximately 38.4°N, 63.8°W, and although it drifted slowly eastward it was assumed stationary (as were the other two buoys). As the IOP-5 storm developed and moved eastward, buoy

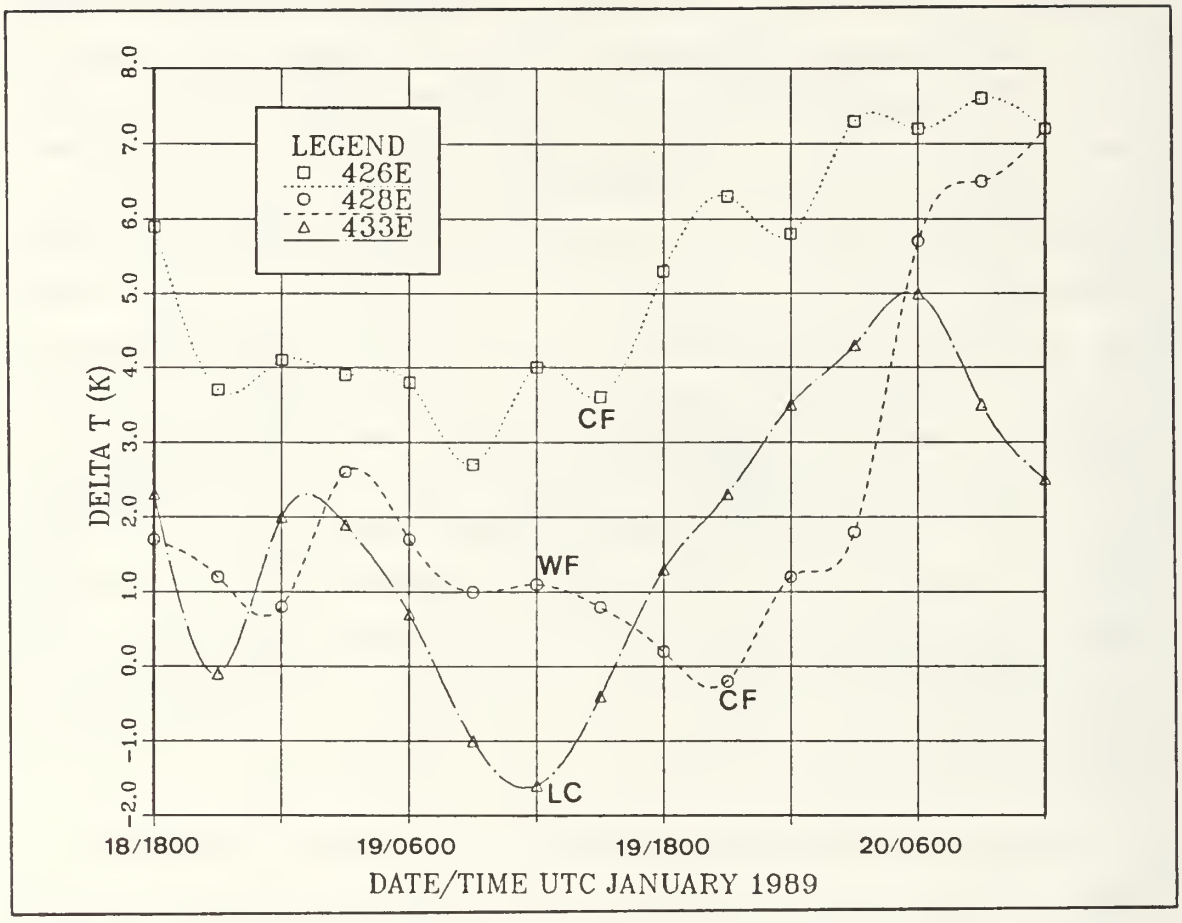

Fig. 26. Buoy Air-Sea Temperature Difference: Buoy 426E was located south of the IOP-5 track while buoy 428E was at the center of the track and 433E was north of the track. CF stands for cold front passage, WF stands for warm front passage and LC stands for low center passage.

426E was initially within the warm sector south of the warm front. At 18/2100 this buoy was located directly east of the location where the IOP-5 storm would develop (The locations of the three buoys are marked with bull's-eyes on the mesoscale analyses, Figs. 4, 7, 8 and 9). The air temperature at the buoy starts out 4° K colder than the sea temperature (Table 3). This buoy stayed within waters where the sea surface temperature remained fairly constant so that the ΔT on the plot can be interpreted as the change in air temperature. As the IOP-5 storm moved eastward buoy 426E remained within the warm sector of the cyclone until the cold front passed at 19/1500. During this period Fig. 26 shows that the air-sea temperature difference remained fairly constant (with the

air colder than the water) except for a small 1° K increase (and subsequent decrease) at 19/0900. This observation supports the previous conclusion that vertical advection offsets the warm advection and positive heat fluxes in the warm sector. Following passage of the cold front the air temperatures decreased steadily causing the ΔT to increase to a maximum of 7° K.

Lilly (1990) also examined the air-sea temperature differences observed at a meteorological buoy located within the warm sector of the IOP-2 cyclone. He found that the air temperature at this buoy increased by 6° K in the 12 h period prior to explosive development and suggested that substantial warming by the surface fluxes contributed to this increase in temperature. The difference between the air-sea temperature difference evolution in the IOP-5 and IOP-2 cyclones may represent the effect of preconditioning. The warm sector air-sea temperature difference is only 4° K in IOP-5 but nearly 12° K in IOP-2, which suggests more preconditioning of the PBL in IOP-5.

Table 3. BUOY 426E AIR-SEA TEMPERATURE DIFFERENCE (South of IOP-5 Track, 38.4°*N*, 63.8°*W*)

Date Time January 1989	Air Temperature (°*K*)	Sea Temperature (°*K*)	ΔT(°*K*)
18/1800	289.6	292.5	5.9
18/2100	288.7	292.4	3.7
19/0000	288.4	292.5	4.1
19/0300	288.5	292.4	3.9
19/0600	288.7	292.5	3.8
19/0900	289.8	292.5	2.7
19/1200	288.5	292.5	4.0
19/1500	289.4	293.0	3.6
19/1800	287.5	292.8	5.3
19/2100	286.5	292.8	6.3
20/0000	286.9	292.7	5.8
20/0300	285.5	292.8	7.3
20/0600	285.8	293.0	7.2
20/0900	285.4	293.0	7.6
20/1200	285.8	293.0	7.2

Table 4. BUOY 428E AIR-SEA TEMPERATURE DIFFERENCE (Center of IOP-5 Track, 40.6°*N*, 57.0°*W*)

Date/Time January 1989	Air Temperature (°*K*)	Sea Temperature (°*K*)	ΔT(°*K*)
18/1800	284.9	286.6	1.7
18/2100	284.9	286.1	1.2
19/0000	285.0	285.8	0.8
19/0300	283.0	285.6	2.6
19/0600	283.9	285.6	1.7
19/0900	284.8	285.8	1.0
19/1200	285.2	286.3	1.1
19/1500	285.8	286.6	0.8
19/1800	286.6	286.8	0.2
19/2100	286.9	286.7	-0.2
20/0000	285.4	286.6	1.2
20/0300	284.5	286.3	1.8
20/0600	281.4	287.1	5.7
20/0900	281.9	288.4	6.5
20/1200	280.7	287.9	7.2

Buoy 428E was located farther east and north of the developing low than the first buoy. As the storm center moved northeastward, this second buoy remained north of the warm front until 19/1200 when the warm front passed. The buoy then remained within the warm sector from 19/1200 until 19/2100 when the cold front passed toward the east. Fig. 26 shows that the air-sea temperature differences at buoy 428E decreased after 19/1200 since the air temperature at the buoy increased slightly with time by approximately 1°K while the buoy remained within the warm sector. Once the cold front passes at 19/2100, Fig. 26 shows increasing air-sea temperature differences when the air temperatures decrease (Table 4) due to cold advection in the cold sector. This buoy (428E) shows a very typical pattern of air-sea temperature differences except that the period of negative air-sea temperature differences (air warmer than the sea) observed while the buoy was in the warm sector was much shorter and weaker than expected. This short

Table 5. **BUOY 433E AIR-SEA TEMPERATURE DIFFERENCE** (North of IOP-5 Track, 41.0°*N*, 63.9°*W*)

Date/Time January 1989	Air Temperature (°*K*)	Sea Temperature (°*K*)	ΔT(°*K*)
18/1800	280.7	283.0	2.3
18/2100	280.0	279.9	-0.1
19/0000	278.2	280.2	2.0
19/0300	279.4	281.3	1.9
19/0600	280.5	281.2	0.7
19/0900	281.4	280.4	-1.0
19/1200	281.3	279.7	-1.6
19/1500	279.8	279.4	-0.4
19/1800	278.3	279.6	1.3
19/2100	278.2	280.5	2.3
20/0000	278.0	281.5	3.5
20/0300	277.5	281.8	4.3
20/0600	278.0	283.0	5.0
20/0900	279.7	283.2	3.5
20/1200	280.7	283.2	2.5

duration may be due to how close the low passed to the buoy. Interestingly, the stability near the low center (buoy 428E) and further south of the warm sector (buoy 426E) differ significantly, with the warm sector being much more unstable.

The third buoy, 433E was located directly north of the first buoy at approximately 41.0°N, 63.9°W. Since the IOP-5 low center passed south of this buoy, both the warm front and the warm sector also passed to the south. Furthermore, this buoy was located near a warm eddy in the Gulf Stream and the fluctuations in sea surface temperature shown in Table 5 indicate that this buoy was probably caught up in the eddy circulation. The sharp fluctuations in ΔT prior to 19/0600 were generated when the air and sea temperatures changed simultaneously but in opposite directions. For example, at 19/0000 an air temperature decrease combined with a sea temperature increase to cause the ΔT to change by 2° K even though the temperature changes in the air and the ocean

were less than 2° K (Table 5). At 19/0600, the well-developed warm front was just south of buoy 433E and the warm front continued to pass to the south until the low center passed south of the buoy at 19/1200. After 19/0600, the air temperature increased by 1° K and the sea temperature decreased by 1.5° K. This change lead to the negative peak that appears at 19/1200. Once the low center passes south of the buoy the air temperature begins to decrease only slightly (less than 2° K) even though the buoy comes under the influence of the cold advection within the cold sector. At the same time, the buoy is evidently being influenced by the warm eddy as the ocean temperature begins to rise dramatically. Consequently, the large increase in the air-sea temperature difference does not strictly represent the influence of cold advection in the atmosphere that is expected. In general, the difference between the air and sea temperatures at this buoy were less than 1.5° K while the buoy was just north of the warm front, which suggests that the PBL north of the warm front was neutral to slightly unstable most of the time.

The analysis in this section confirms that the changes in the surface air temperatures were much smaller than expected. Temperatures within the warm sector remained fairly constant in spite of the strong positive heat fluxes and warm advection that characterize this region. Furthermore, the small differences in air-sea temperatures north of the warm front indicate a neutral to slightly unstable PBL in this area. These features suggest that convective processes within the warm sector and along the warm front are transporting heat and moisture away from the PBL. West of the cold front the increasing air-sea temperature differences are consistent with the falling temperatures expected to result from cold advection. This analysis also demonstrates that mesoscale features, such as the Gulf Stream warm eddy in the vicinity of buoy 433E, may strongly influence the thermal structure of the PBL.

D. EVALUATION OF IOP-5 MOIST SYMMETRIC NEUTRALITY

Because the PBL in the warm sector is characterized by positive fluxes and strong vertical transport, the potential for coupling between the boundary layer and the middle troposphere is significant in the IOP-5 storm. As discussed in the previous section, the 19/0001 GOES IR imagery (Fig. 18) shows a region of convective clouds directly above a region of positive heat fluxes in the warm sector, which suggests that destabilization of the surface layer has contributed to deep convection and provides qualitative evidence for this coupling. Several previous studies have suggested that the boundary layer forces convection or slantwise convection in the warm frontal region since this region is possibly characterized by moist symmetric instability. As discussed in the backround chapter,

the studies by Nuss and Kamikawa (1990) and Kuo et al. (1991) support the idea that moist symmetric neutrality may be a charactistic feature of explosively deepening storms.

The sounding and dropsonde data available for IOP-5 were examined to determine times when the data were sufficient to construct cross sections that would allow an assessment of whether conditions of moist symmetric neutrality in the warm front region of IOP-5 support this type of direct coupling. Data were available to construct two sections across the warm front for the 19/0600 and 19/0900 times. Psuedo-angular momentum M for a north-south cross section was defined as $M = u - fy$, following Emanuel (1983) where u is the zonal velocity, f is the coriolis parameter and y is the distance from the southern-most sounding. Fig. 27 shows a θ_e vs. M cross section for 19/0600, and Fig. 28 shows a cross section for 19/0900. Locations of the cross sections in relation to the warm front at 19/0600 and 19/0900 are shown in Fig. 12 and Fig. 19, respectively. Both cross sections show some indication of moist symmetric neutrality as indicated by the parallel θ_e and M-lines in the warm frontal regions, however the baroclinic zone of the warm front in these sections is not very strong, and the θ_e and M-lines are not parallel all the way to the surface indicating regions of both stable (slope of θ_e-lines less than slope of M-lines) and unstable slantwise stratification. Neither of the cross sections were strictly oriented north-south and consequently the u-velocity component is only an estimate of the shear in the plane of the cross sections, which may account for the lack of absolute moist symmetric neutrality. In addition, the three-dimensional nature of the frontal regions limits the applicability of this theory based on the two-dimensionality of fronts. However, the fact that convection is observed in the satellite imagery suggests that vertical or slantwise instability is present in the warm frontal region of IOP-5.

Given this potential for coupling between the surface layer and the middle troposphere through vertical or slantwise convection, the positive sensible heat fluxes east of the IOP-5 low would destabilize the atmosphere along the warm front. The same positive heat and moisture fluxes (IOP-5 moisture fluxes are assumed to follow the heat flux pattern) would fuel convective transport of heat and moisture and enhance upper level latent and sensible heating. This pattern would enhance both vertical and slantwise convection, but the existence of symmetric neutrality within the warm front suggests that slantwise convective adjustment has neutralized an unstable environment. Moreover, the continued presence of positive heat fluxes in the warm frontal region accom-

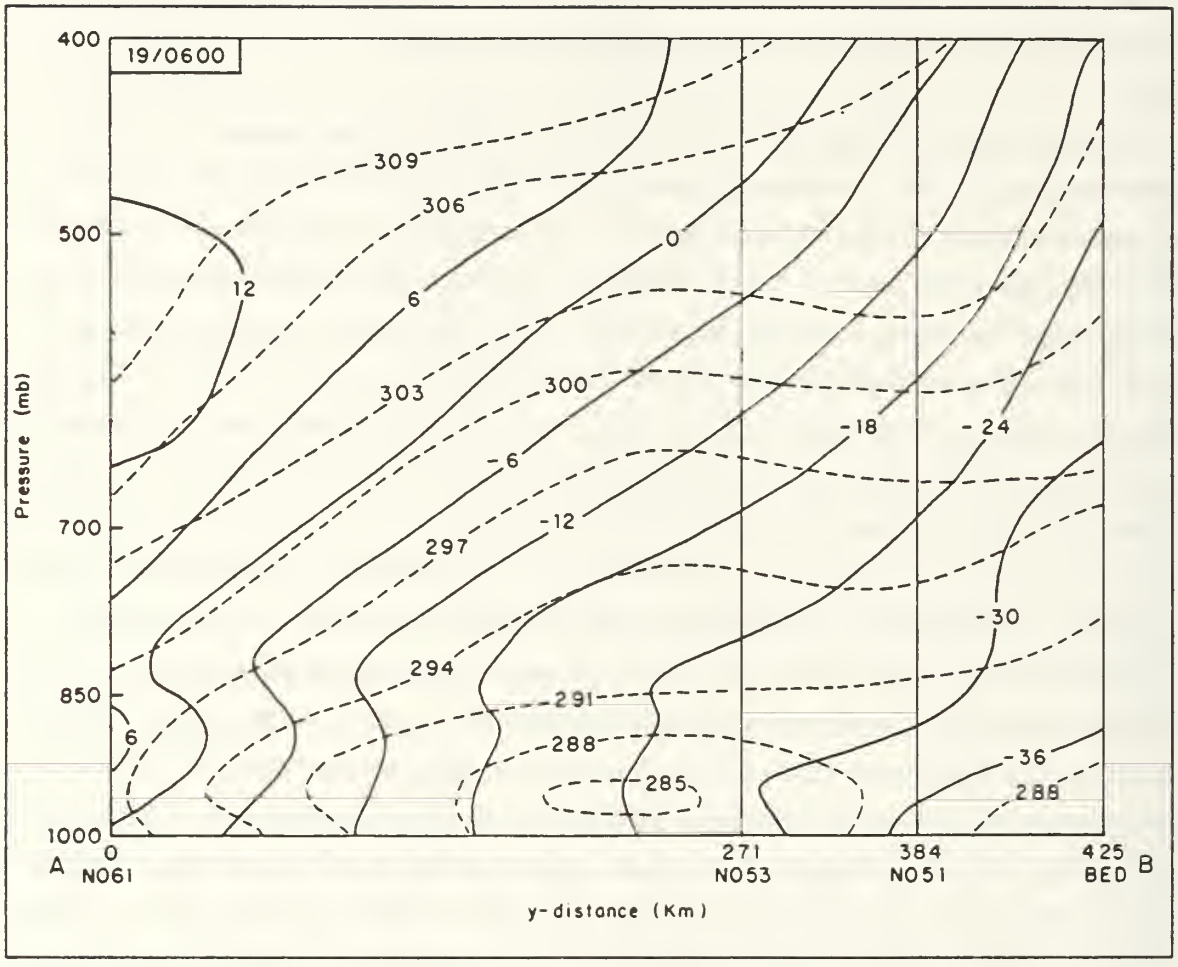

Fig. 27. Cross Section at 19/0600 UTC January 1989: Equivalent potential temperature θ_e (dashed) in 3° K intervals and pseudoangular momentum M (solid) in 6 m s^{-1} intervals across the IOP-5 warm front.

panied by the strong evidence of upward heat transport would provide the forcing needed to maintain slantwise convection.

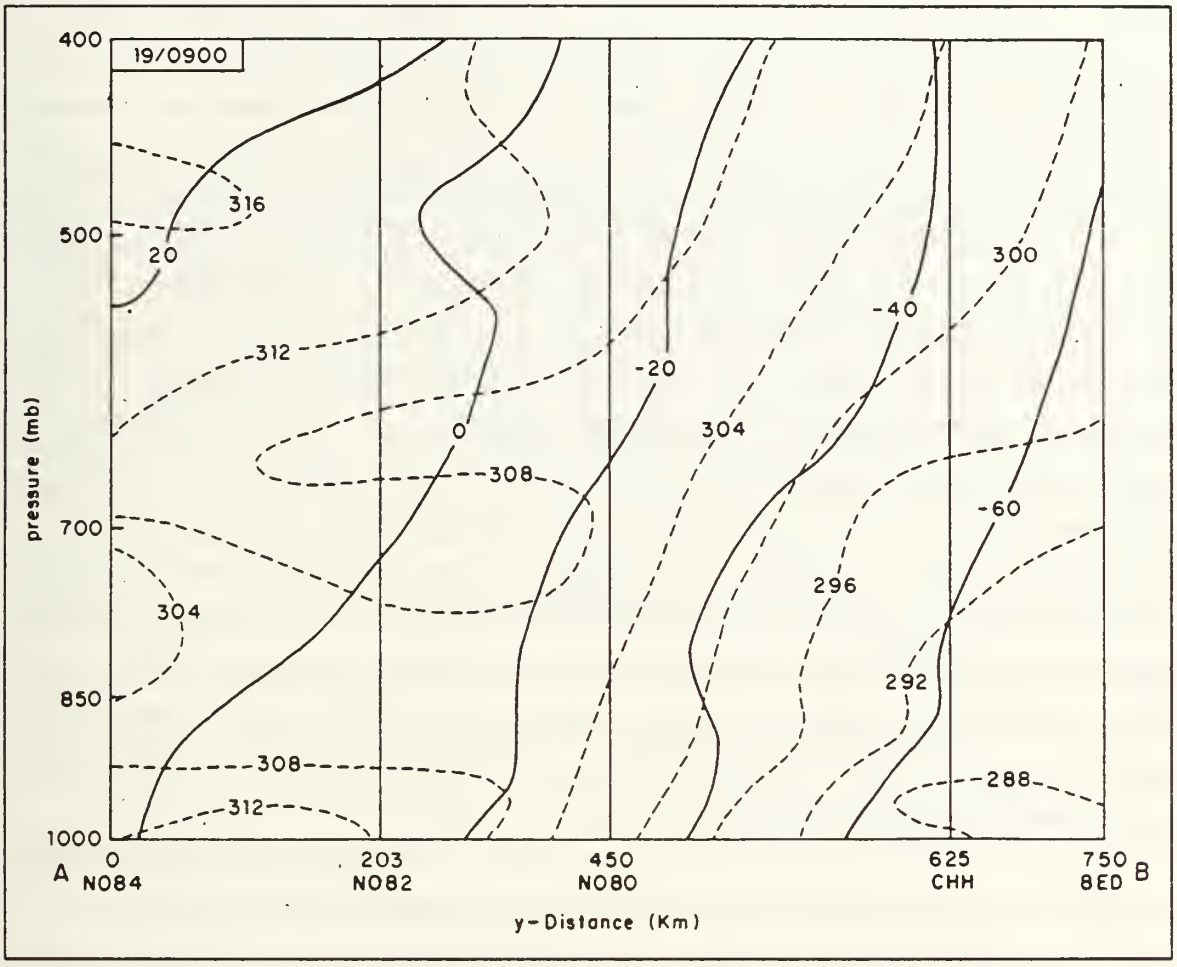

Fig. 28. Cross Section at 19/0900 UTC January 1989: Equivalent potential temperature θ_e (dashed) in 4° K intervals and pseudoangular momentum M (solid) in 20 m s^{-1} intervals across the IOP-5 warm front.

VI. CONCLUSIONS AND RECOMMENDATIONS

Analysis of the synoptic forcing associated with development of the IOP-5 storm revealed many features that were characteristic of typical cyclone development. For example, the location of a 500 mb shortwave trough upstream of the developing surface low generated upper-level divergence favorable to cyclogenesis. The upper-level divergence was further enhanced by the significant upper-level diffluence generated by 300 mb jets that diverged north and south of the developing low. It would be tempting to conclude that simply increasing the strength of the synoptic forcing leads to explosive cyclogenesis, but if this were true the same model that provides a good forecast for a typical storm should also provide a good forecast for an explosively deepening storm. In general, this has not been the case, but there is some indication that model resolution may also be a key factor, since models with finer resolution generally provide a better forecast for explosively deepening storms. Still, the record of poor model forecasts for explosively deepening storms suggests that some distinct characteristics of these storms are not being captured by the models.

In order to examine the IOP-5 storm more closely, a detailed mesoscale analysis was completed. This analysis showed that the IOP-5 storm deepened explosively at a maximum rate of 32 mb over a 24 h period. Both the IOP-5 storm and the IOP-2 storm (Lilly, 1990) were characterized by a 9 h period of rapid deepening that was preceeded and followed by periods of more moderate deepening. This pattern suggests a build-up in the forcing that leads to a maximum explosive deepening rate, followed by more moderate deepening once the forcing has been spent.

The most significant feature that distinguishes the IOP-5 cyclone from the typical cyclone model is the existence of positive heat fluxes east of the low center that destabilize the boundary layer and enhance low level baroclinicity associated with the warm front. In contrast, warm advection into the warm sector of a typical cyclone would be expected to create conditions where warm air above the cooler ocean would establish negative heat fluxes that would increase stability and decrease baroclinicity along the warm front. The "atypical" pattern of positive heat fluxes that characterizes the warm sector of the IOP-5 storm is clearly one factor that contributed to explosive cyclogenesis of this storm. Furthermore, the lack of boundary layer temperature changes in the warm sector indicates that heat and moisture are are being transported away from the bound-

ary layer, resulting in coupling of the surface processes to the middle and upper troposphere. Further evidence of this coupling is suggested by the conditions of moist symmetric neutrality observed in the warm frontal region. The continuous positive fluxes within the warm sector of the IOP-5 storm could provide the forcing needed to maintain moist slantwise convection that would neutralize an unstable atmosphere and lead to the conditions of moist symmetric neutrality observed in the IOP-5 cross sections.

Several other features also contributed to enhanced cyclogenesis. The Gulf Stream SST gradient strongly influenced development of the IOP-5 storm. This influence was evident throughout cyclone development since the 3 hourly plots of the air-sea temperature differences in the vicinity of the storm closely resembled the Gulf Stream SST gradient. Furthermore, the track of the IOP-5 storm paralleled this gradient, causing the storm to remain in a region characterized by cooler air temperatures above the warmer waters south of the Gulf Stream. This relationship of air-sea temperature differences initiated the positive heat fluxes that existed throughout the region south of the Gulf Stream. Additionally, cold advection associated with a preexisting storm to the northeast of the region where the IOP-5 storm developed probably helped force cold air south of the Gulf Stream. This source of cooler air helped maintain the positive heat fluxes above the Gulf Stream as well as allowing preconditioning of the atmosphere to take place prior to IOP-5 development.

The previous discussion shows evidence that many features contributed to generating the strong forcing that resulted in explosive cyclogenesis of the IOP-5 storm. The most significant feature of this storm was the continuous positive heat fluxes that occurred east of the low center. Although this feature has been observed in several explosive cyclone studies, and has generated deeper cyclones in model studies, it is not characteristic of all explosive deepening storms. Results of the mesoscale analysis of IOP-5 suggest that further studies of explosive cyclogenesis are necessary to to establish, if possible, the characteristic features of these storms. The following recommendations are proposed for future studies:

1. Continue to analyze the boundary layer dynamics of explosively deepening storms in order to establish features that distinguish them from nonexplosive storms.
2. Compare the surface analyses of the IOP-5 storm to the upper level analyses and determine the relationship between surface and upper level forcing.
3. Complete upper-level analyses to completely diagnose stability in the warm front and the vertical transport of heat and moisture in the warm sector.
4. Conduct model studies that include slantwise convection in order to assess its contribution to cyclone development.

5. Analyze surface moisture and wind fields to evaluate the contribution of latent heat fluxes and frictional convergence to the boundary layer dynamics.

VII. REFERENCES

Bjerknes, J., 1919: On the structure of moving cyclones. *Geofys. Publ.*, **1**, No. 2, 8 pp.

_____, and H. Solberg, 1922: Life cycle of cyclones and the polar front theory of atmospheric circulation. *Geofys. Publ.*, **3**, No. 1, 30-45.

Brown, R. A. and W. T. Liu, 1982: An operational large-scale marine planetary boundary layer model. *J. Appl. Meteor.*, **21**, 261-269.

Cressman, G. R., 1959: An operational objective analysis system. *Mon. Wea. Rev.*, **87**, 367-374.

Davis, C. A., and K. A. Emanuel, 1988: Observational evidence for the influence of surface heat fluxes on rapid maritime cyclogenesis. *Mon. Wea. Rev.*, **116**, 2649-2659.

Emanuel, K. A., 1983: On assessing local conditional symmetric instability from atmospheric soundings. *Mon. Wea. Rev.*, **111**, 2016-2033.

_____, 1988: Observational evidence of slantwise convective adjustment. *Mon. Wea. Rev.*, **116**, 1805-1816.

Fantini, M., 1990: The influence of heat and moisture fluxes from the ocean on the development of baroclinic waves. *J. Atmos. Sci.*, **47**, 840-855.

Fleagle, R. G., and W. A. Nuss, 1985: The distribution of surface fluxes and boundary layer divergence in midlatitude ocean storms. *J. Atmos. Sci.*, **42**, 784-799.

_____, N. A. Bond, and W. A. Nuss, 1988: Atmosphere-ocean interaction in midlatitude storms. *Meteor. Atmos. Phys.*, **38**, 50-63.

Hadlock, R., and C. W. Kreitzberg, 1988: The experiment on rapidly intensifying cyclones over the Atlantic (ERICA) field study: Objectives and plans. *Bul. Am. Met. Soc.*, 69, 1309-1320.

Kuo, Y. H., R. J. Reed, and S. Low-Nam, 1991: Effects of surface energy fluxes during the early development and rapid intensification stages of seven explosive cyclones in the western Atlantic. *Mon. Wea. Rev.*, 119, 457-476.

_____, and S. Low-Nam, 1990: Prediction of nine explosive cyclones over the western Atlantic ocean with a regional model. *Mon. Wea. Rev.*, 118, 3-25.

Lilly, C. D., 1990: Mesoscale surface analyses of the ERICA IOP-2 cyclone. Master's Thesis, Naval Postgraduate School, Monterey, CA, 64 pp.

Neiman, P. J., M. A. Shapiro, E. G. Donall, and C. W. Kreitzberg, 1990: Diabatic modification of an extratropical marine cyclone warm sector by cold underlying water. *Mon. Wea. Rev.*, 118, 1576-1590.

Nuss, W. A., 1989: Air-sea interaction influences on the structure and intensification of an idealized marine cyclone. *Mon. Wea. Rev.*, 117, 351-369.

_____, and R. A. Anthes, 1987: A numerical investigation of low-level processes in rapid cyclogenesis. *Mon. Wea. Rev.*, 115, 2728-2743.

_____ and S. I. Kamikawa, 1990: Dynamics and boundary layer processes in two Asian cyclones. *Mon. Wea. Rev.*, 118, 755-771.

Palmén, E., and C. W. Newton, 1969: *Atmospheric Circulation Systems, Their Structure and Physical Interpretation.* Academic Press, 603 pp.

Reed, R. J., and M. D. Albright, 1986: A case study of explosive cyclogenesis in the eastern Atlantic. *Mon. Wea. Rev.*, 114, 2297-2319.

Sanders, F., 1986: Explosive cyclogenesis in the West-Central North Atlantic ocean, 1981-84. Part I: Composite structure and mean behavior. *Mon. Wea. Rev.*, **114**, 1781-1794.

_____, 1987: Skill of NMC operational dynamical models in predicting explosive cyclogenesis. *Wea. Forecasting*, **2**, 322-336.

_____, 1989: Surface pressure and temperature analysis for the Experiment on Rapidly Intensifying Cyclones over the Atlantic (ERICA) Intensive Observation Periods (IOPs). (Available from ERICA Data Center, Department of Physics and Atmospheric Science, Drexel University, Philadelphia, PA.)

_____, 1990: Surface analysis over the oceans - searching for sea truth. *Wea. Forecasting*, **5**, 596-612.

_____, and J. R. Gyakum, 1980: Synoptic-dynamic climatology of the "bomb". *Mon. Wea. Rev.*, **108**, 1589-1606.

Ucellini, L. W., 1986: The possible influence of upstream upper-level baroclic processes in the development of the QE II storm. *Mon. Wea. Rev.*, **114**, 1019-1027.

_____, D. Keyser, K. F. Brill, and C. H. Wash, 1985: The Presidents' Day cyclone of 18-19 February 1979: Influence of upstream trough amplification and associated tropopause folding on rapid cyclogenesis. *Mon. Wea. Rev.*, **113**, 962-988.

VIII. INITIAL DISTRIBUTION LIST

		No. Copies
1.	Defense Technical Information Center Cameron Station Alexandria, VA 22304-6145	2
2.	Library, Code 52 Naval Postgraduate School Monterey, CA 93943-5002	2
3.	Chairman (Code MR Hy) Department of Meteorology Naval Postgraduate School Monterey, CA 93943-5000	1
4.	Professor Wendell A. Nuss (Code MR/Nu) Department of Meteorology Naval Postgraduate School Monterey, CA 93943-5000	2
5.	Professor Pat Pauley (code MR/Pa) Department of Meteorology Naval Postgraduate School Monterey, CA 93943-5000	1
6.	LT Susan N. Greer Naval Oceanography Command Facility Box 26 FPO New York, NY 09571-0926	
7.	Commander Naval Oceanography Command Stennis Space Center MS 39529-5000	1
8.	Commanding Officer Fleet Numerical Oceanography Center Monterey, CA 93943-5005	1
9.	Commanding Officer Naval Oceanographic and Atmospheric Research Laboratory Stennis Space Center MS 39529-5004	1
10.	Director Naval Oceanographic and Atmospheric Research Laboratory Monterey, CA 93943-5006	1

11. Chief of Naval Research
800 North Quincy Street
Arlington, VA 22217 — 1

12. Office of Naval Research
Naval Ocean Research and Development Activity
800 N. Quincy Street
Arlington, VA 22217 — 1

Thesis
G7565 Greer
c.1 Mesoscale surface
analysis of the ERICA
IOP-5 cyclone.

Thesis
G7565 Greer
c.1 Mesoscale surface
analysis of the ERICA
IOP-5 cyclone.

DUDLEY KNOX LIBRARY
3 2768 00016381 0